Non-canonical Activation of Human Group 2 Innate Lymphoid Cells by TLR4 Signaling

Li She[1,2], Hamad H. Alanazi[1], Jingwei Wang[1,6], Daniel P. Chupp[1], Yijiang Xu[1], Hong Zan[1], Zhenming Xu[1], Yilun Sun[1], Na Xiong[1], Nu Zhang[1], Xin Zhang[2,3,4,5], Yong Liu[2,3,4,5*], and Xiao-Dong Li[1*]

[1]Department of Microbiology, Immunology and Molecular Genetics
Long School of Medicine
University of Texas Health San Antonio
San Antonio, TX 78229-3900

[2]Department of Otolaryngology-Head and Neck Surgery,
[3]Clinical Research Center for Pharyngolaryngeal Diseases and Voice Disorders,
[4]Otolaryngology Major Disease Research Key Laboratory of Hunan Province
[5]National Clinical Research Center for Geriatric Disorders, Xiangya Hospital
[6]Institute of Pediatrics, The Second Xiangya Hospital
Central South University
Changsha, Hunan 410008
China

[*]Correspondence: liuyongent@csu.edu.cn

lix8@uthscsa.edu

Running Title: **Non-canonical activation of human ILC2 cells by TLR4**

KEYWORDS AND ABBREVIATIONS
group 2 innate lymphoid cells (ILC2); toll-like receptor 4 (TLR4); lipopolysaccharides (LPS); interleukin 33 (IL-33); Interleukin 1 receptor-like 1 (IL1RL1, also called IL-33R or ST2); interleukin 4 (IL-4); interleukin 5 (IL-5); interleukin 13 (IL-13).

Abstract

Group 2 innate lymphoid cells (ILC2) are emerging as a critical player in type 2 immunity at barrier sites in response to microbial infections and allergen exposures. Although their classical activators are known to be host epithelial-derived alarmin cytokines IL-33, IL-25 or TSLP, it remains elusive whether ILC2 cells can be activated by directly sensing microbial ligands via pattern-recognition receptors such as toll-like receptors (TLRs). Here we report that toll-like receptor 4 (TLR4) is a potent activating receptor of human ILC2. We found that among many microbial ligands examined, lipopolysaccharides (LPS) from multiple species of Gram-negative bacteria, was found to potently stimulate human, but not murine ILC2, to proliferate and produce massive amounts of type 2 effector cytokines IL-4, IL-5, and IL-13. LPS-activated ILC2 also had greatly enhanced the CD40 ligand (CD154) expression and were able to promote the proliferation and antibody production of human B cells in culture. In a humanized mouse model, LPS activated the adoptively transferred human ILC2 in mouse lungs. Both NF-kB and JAK pathways, but not the IL-33-ST2 pathway, were required for LPS to activate human ILC2. RNA-seq data further revealed that LPS induced a large set of genes overlapped significantly with those induced by IL-33. Collectively, these findings support a non-classical mode of activating human ILC2 cells via the LPS-TLR4 signaling axis. Thus, targeting TLR4 signaling pathway might be developed as a new approach by modulating ILC2 activation in treating various type 2 immunity-associated diseases.

Introduction

Allergic disorders including asthma, allergic rhinitis and atopic dermatitis (AAA) are common diseases affecting more than 300 million people worldwide (Jackson et al., 2013; Kay, 2001a; Kay, 2001b). Although AAA diseases are traditionally characterized by an overzealous Th2-mediated inflammatory response, it has become increasingly appreciated in recent years that group 2 innate lymphoid cells (ILC2) play an important role in the initiation and orchestration of type 2 immunopathologies (Vivier et al., 2018). ILC2 cells are the innate counterparts of Th2 lymphocytes, but lack rearranged antigen receptors (Artis and Spits, 2015; Barlow and McKenzie, 2019; Eberl et al., 2015; Vivier et al., 2018). In response to three classical activators, alarmin cytokines IL-33, IL-25 and TSLP, ILC2 cells can promptly produce huge amounts of type 2 effector cytokines such as IL-5 and IL-13, which drive the development of type 2 immunopathologies featured by eosinophilia, airway remodeling and mucus hypersecretion (Cayrol and Girard, 2018; Kubo, 2017; Liew et al., 2016; Molofsky et al., 2015).

In reality, environmental allergens are very complex and often contaminated with microbial or parasitic products such as lipopolysaccharide (LPS), also known as endotoxin, or chitin, so called pathogen-associated molecular patterns (PAMPs). PAMPs could stimulate innate immune cells through binding and activating their corresponding pattern recognition receptors (PRRs). Besides sensing PAMPs, PRRs can also recognize self-ligands, namely, DAMPs (damage-associated molecular patterns) (Akira et al., 2006; Brubaker et al., 2015; Man et al., 2016; Wu and Chen, 2014). Toll-like receptors (TLRs) are the first class of PRRs. All TLRs contain extracellular leucine-rich repeats (LRRs) for ligand bindings and an intracellular Toll-interleukin-1 receptor (TIR) domain that recruits MyD88 and other adaptor proteins to activate signaling cascades, which culminate in the production of various pro- or anti-inflammatory cytokines. To date, 10 TLRs (TLR1–10) have been identified in humans and 12 (TLR1–9, TLR11–13) in mice (Roach et al., 2005). TLR2 forms a heterodimer with TLR1, TLR6 or TLR10 to detect microbial lipopeptides and peptidoglycans. TLR4 detects bacterial LPS while TLR5 recognizes bacterial flagellin. The nucleic acid sensing TLRs include TLR3, TLR7/8, TLR9 and TLR13, which detect double-stranded RNA (e.g. poly[I:C]), R848 or single-stranded RNA (ssRNA), unmethylated CpG DNA (e.g. CpG-A), bacterial 23S rRNA and its derivative, a 13-nt sequence, ISR23, respectively (Li and Chen, 2012).

The immune activation of allergen-associated PAMPs is believed to be critically involved in the initiation of allergic type 2 inflammation (Locksley, 2010; Palm et al., 2012; Stewart and Thompson, 1996; Van Dyken et al., 2011; Van Dyken et al., 2017; Van Dyken et al., 2014). Recent studies have also demonstrated that microbial ligands can activate the corresponding innate immune receptors to protect against eosinophilic airway diseases through inhibition of ILC2 function(Maazi et al., 2018; Sabatel et al., 2017; Thio et al., 2019). TLR4 was previously shown to play a role in regulating type 2 immune responses in mouse studies, however, the underlying mechanism of action remains poorly understood (Deckers et al., 2017; Eisenbarth et al., 2002; Hammad et al., 2009; Hammad and Lambrecht, 2015; McAlees et al., 2015; Trompette et al., 2009). Although the role of pattern-recognition receptors (PRRs) in myeloid cells like monocytes and DCs is well established, it remains unclear whether PRRs such as TLRs can directly function in ILC2 cells.

In the course of investigating the ability of ILC2 cells to respond to various TLR ligands, we found that only LPS was able to robustly trigger human, but not murine ILC2 cells, to proliferate and produce type 2 effector cytokines including IL-4, IL-5, and IL-13. Further, LPS treatment greatly enhanced CD40 ligand (CD154) expression on ILC2 cells to promote the proliferation and antibody production of human B cells. Adoptive cell transfer experiments using humanized mouse models showed that LPS can activate

human ILC2 cell in vivo in mouse lungs. Moreover, RNA-seq data revealed that LPS induced a large set of genes overlapped with those induced by IL-33. Collectively, these findings support a non-classical mode of activating human ILC2 cells by the LPS-TLR4 signaling axis.

Results

LPS potently activates the proliferation and cytokine production of human, but not murine ILC2 cells

ILC2 cells are known to be primarily activated by alarmin cytokines IL-33, TSLP or IL-25. However, it remains elusive whether ILC2 cells are capable of directly sensing microbial products through PRRs such as TLRs. To address this issue, various TLR agonists were initially used to examine their abilities to activate in vitro-cultured human (CD45+Lin-CRTH2+CD127+) or murine (CD45+Lin-T1/ST2+) ILC2 cells, which were originally isolated from human blood or murine lung samples by FACS sorting (**Fig. S1**). The growth and cytokine production of ILC2 cells were analyzed on day 3 (**Fig. S2**) and 5 (all experiments if not indicated) with techniques including microscopic examinations, FACS and ELISA, respectively. Among a number of TLR ligands tested, LPS (*E. coli* 0127:B8) was identified to potently stimulate human, but not murine, ILC2 cells to proliferate (**Figs. 1A & B and 1D & E**), and produced massive amounts of type 2 effector cytokines IL-5 and IL-13 (**Figs. 1C and 1F**). Pam3CSK4, a TLR2 agonist, was very toxic to human ILC2 cells, but seemed to be stimulatory to murine ILC2 cells (**Figs. 1D, E & F**). Interestingly, at a proper concentration range, Pam3CSK4 stimulated both human (0.01-0.1 μg/ml) and murine (1-10 μg/ml) ILC2 cells (**Fig. S3**), which is consistent with previous reports (Crellin et al., 2010; Ishii et al., 2019). In addition, LPS from three Gram-negative bacteria including *E. coli* 055:B5, *P. aeruginosa* and *S. typhimurium* was also found to strongly activate human ILC2 cells (**Fig. S4**). LPS activated human ILC2 cells in a concentration-dependent manner (**Fig. 2**) and promoted their survivals even at the highest concentration (100 μg/ml) (**Fig. S5**). We also carefully examined the effects of LPS at different concentrations on murine ILC2 cells and found that LPS at 10 or 100 μg/ml did have some weak stimulating effects on murine ILC2 cells **(Fig. S6)**. Taken together, these data suggested that at proper concentrations, LPS has the ability to directly activate human, but not murine ILC2 cells, to proliferate and induce the secretion of type 2 effector cytokines IL-5 and IL-13.

LPS activates human ILC2 cells via TLR4 receptor without the involvement of IL-33-ST2 pathway

Next, we investigated the involvement of TLR4- and ST2-mediated pathways in LPS-triggered signaling in human ILC2 cells. Although it was reported that human ILC2 cells expressed TLR4 mRNA and responded to a Mix of TLR-ligands (Maggi et al., 2017), it remains to be determined whether LPS alone can act on TLR4 signaling in human ILC2 cells. To address this question, we first analyzed the protein expression level of TLR4 and its co-receptor CD14 in ILC2 cells derived from 4 healthy donors. FACS staining showed that TLR4, but not CD14, was detected on the surfaces of unstimulated ILC2 cells from all 4 donors (**Fig. 3A**). Functionally, LPS strongly enhanced the growth of ILC2 cells derived from all 4 donors at various degrees. Notably, LPS could even significantly increase the effects of IL-33 on the proliferation of ILC2 cells derived from 3 donors (**Figs. 3B & C**). LPS alone triggered the cytokine production of IL-5 and IL-13 by ILC2 cells derived from all 4 donors (**Fig. 3D**). Chemically, LPS contains three parts: lipid A, O-antigen and core oligosaccharide joined by a covalent bond. Lipid A domain is responsible for the toxicity of Gram (-) bacteria and binding to TLR4. To determine a specific role of TLR4 receptor in LPS-mediated activating human ILC2 cells, we used a chemically synthesized TLR4 agonist a lipid A analog (CRX-527) (Stover et al., 2004) and an natural antagonist, LPS-RS, to stimulate or block TLR4-specific signaling, respectively. Given that the CRX-527 solvent DMSO at higher concentrations is toxic to cells, DMSO alone at different concentrations was included as a control

145 to rule out its compound effects on ILC2 cells (**Fig. 4A**). CRX-527 at 0.1 and 1 μg/ml strongly promoted
146 the growth (**Fig. 4A & B**) and the production of IL-5 and IL-13 (**Fig. 4C**). Due to the toxic effects of
147 DMSO, CRX-527 at higher concentrations 10 or 100 μg/ml completely lost its stimulating effects. Next,
148 we asked whether the LPS activity could be competitively blocked LPS-RS, a lipopolysaccharide isolated
149 from the photosynthetic bacterium, *Rhodobacter sphaeroides*, which is known to be unable to induce
150 TLR4 signaling (Coats et al., 2005). Remarkably, LPS-RS at 50 μg/ml or above almost completely
151 inhibited the biological effects of LPS. It is worth to mention that both LPS and LPS-RS were dissolved
152 in water (**Fig. 4D, E & F)**. To further address the possible involvement of IL-33-ST2 pathway, we
153 performed a competitive assay by adding increased amounts of the recombinant protein IL1RL1 into
154 ILC2 culture in order to sequester free IL-33. It turned out that whereas IL1RL1 at 1 and 10 μg/ml
155 significantly blocked the effects of IL-33, it failed to affect the activity of LPS on human ILC2 cells (**Fig**
156 **5A, B & C**). These results indicate that LPS activates human ILC2 cells via TLR4 receptor without the
157 involvement of IL-33-ST2 pathway.
158
159 **RNA-seq analysis reveals that LPS-induced genes overlap significantly with those induced by IL-**
160 **33 in human ILC2 cells**
161 We wanted to obtain a global view on the LPS-activated human ILC2 cells at the transcriptional level. In
162 order to find the best timepoint to collect samples for the RNA-seq analysis, we examined the kinetics of
163 selected genes (IL-4, IL-5, IL-13 and TNFα) induced by LPS in comparison to an IL-33 control by RT-
164 qPCR. We found that the peak level of these genes appeared at 6 hours in both treatments (**Fig. S7**).
165 Therefore, we chose the 6h samples to perform an RNA sequencing analysis (**Fig. 6**). We first compared
166 the relative mRNA expression level of all human TLRs and found that TLR4 was the highest expressed
167 gene in non-treated human ILC2 cells, suggesting the importance of TLR4 signaling in this cell type (**Fig.**
168 **6A**). Next, we analyzed the differential expression of all genes. In a volcano-plot analysis, 213 genes
169 were up-regulated whereas 52 genes were down-regulated compared with the control, which can be also
170 seen in a heatmap analysis (**Fig. 6B & C**). More interestingly, further cytokine analysis found that many
171 type 2 effector cytokines such as IL-5, IL13 and CSF2 were induced and highlighted in red (**Fig. 6D**). To
172 further define the functional connections of the DFGs genes, the KEGG (Kyoto Encyclopedia of Genes
173 and Genomes) pathway enrichment and GOBP (Gene Ontology Biological Process) analyses were
174 performed. We discovered that genes from the LPS-treated sample were significantly enriched in
175 biological processes highly related to immune modulations by cytokines such as TNF and IL-17 (**Figs.**
176 **6E & S8**). By a direct comparison using gene set enrichment analysis (GSEA), IL-33-upregulated gene
177 set was identified to be statistically significant concordance with those induced by LPS (**Fig. 6F**), sharing
178 more than 50% genes (141 genes) (**Fig. 6G**). Taken together, these results reveal that LPS-induced genes
179 overlap significantly with the gene signature induced by IL-33 in human ILC2 cells.
180
181 **NF-κB and JAK-STAT pathways are critical for LPS to activate human ILC2 cells**
182 Given that the engagement of TLRs often triggers the common signaling cascades leading to the
183 activation of a number of transcription pathways (Kaisho and Akira, 2006), we wanted to know which
184 pathway is required for LPS to activate human ILC2 cells. To this end, we performed additional RNA-
185 seq analysis and found that the NF-κB and JAK-STAT signaling pathways were strongly associated with
186 the function of LPS-activated human ILC2 cells **(Fig. 7A).** Next, we wanted to determine whether the
187 NF-κB or JAK inhibitors would affect the growth and cytokine production of human ILC2 cells treated
188 with LPS. As expected, NF-κB inhibition with Bay 11-7082 at the concentration between 1 to 100 μM
189 completely blocked the LPS-mediated stimulating effects. A pan-Jak inhibitor also blocked all responses
190 to LPS (**Figs. 7B, C & D**). Similarly, these two inhibitors also blocked IL-33-mediated effect on ILC2

191 cells (**Figs. 7E, F & G**). These data indicate that the NF-κB- and JAK-dependent pathways contribute
192 significantly to LPS -mediated activation of human ILC2 cells.
193
194 **LPS-activated ILC2 cells promote the proliferation and antibody production of B cells**
195 It has been recently shown that ILC2 can interact with other cell types such as DCs, Th2 or B cells to
196 bridge the innate and adaptive immunity (Drake et al., 2016; Gurram and Zhu, 2019; Halim et al., 2016;
197 Maggi et al., 2017; Moon et al., 2004). We wondered whether LPS-activated ILC2 cells could activate
198 naïve B cells. Notably, it is generally believed that LPS is unable to directly activate human B cell because
199 its receptor TLR4 expression of human B cell is very low (Bourke et al., 2003; Ganley-Leal et al., 2010).
200 Since we have shown above that LPS-activated human ILC2s increased the mRNA or protein expression
201 of a few B cell regulatory factors including CD40LG (CD154), IL-5 and IL-13 (**Figs. 3D & 6D**)
202 (Defrance et al., 1994; Moens and Tangye, 2014; Moon et al., 2004), we then asked whether the LPS-
203 activated human ILC2s cells could activate naïve B lymphocytes by producing other B cell stimulating
204 factors at the protein level such as CD154 and IL-4, which are required for the antibody class switching.
205 Indeed, the CD154 expression and the secretion of IL-4 by ILC2 cells from all 4 donor was greatly
206 induced after the treatment with either LPS or IL-33 (**Figs. 8A & B**). To further prove that LPS-treated
207 human ILC2s were able to induce the antibody production of human B cells, we purified human B cells
208 ($CD19^+$ cells). As illustrated in **Fig. 8C**, ILC2s cells were cocultured with B cells at the 1:1 ratio in the
209 absence or presence of LPS, respectively. After 5 days, the number of B cells and levels of IgM, IgG,
210 IgA and IgE present in culture supernatants were measured. As shown in **Figs. 8D & E**, LPS-stimulated
211 ILC2 activated B cells to proliferate and produce high levels of antibodies including IgM, IgG, IgA and
212 IgE. Unstimulated ILC2 cells failed in inducing the growth and immunoglobulin production of B cells.
213 Collectively, these results suggest that LPS-TLR4 signaling in human ILC2 is sufficient to activate the
214 proliferation and antibody production of human B cells.
215
216 **LPS induces human ILC2 cells-mediated eosinophilic lung inflammation in vivo**
217 Since we have shown that LPS is a potent ILC2 activator in vitro, we next moved on to evaluate whether
218 LPS was able to elicit human ILC2 cells-mediated eosinophilia in vivo. To this end, we developed two
219 humanized mouse models, in which NSG or $Rag2^{-/-}\gamma c^{-/-}$ mice were reconstituted with human ILC2s as
220 illustrated in **Fig. 9A**. Similar models have recently been reported with the IL-33 administration (Crellin
221 et al., 2010; Hurrell et al., 2019). Due to a high level of protein sequence homology, human IL-5 could
222 function as murine IL-5 and was previously used to activate murine eosinophils (Ingley et al., 1991;
223 Tavernier et al., 1995). Consistent with our in vitro data, human ILC2 cells in mouse lung responded to
224 LPS stimulations, which led to increased number of murine lung eosinophils in both NSG or $Rag2^{-/-}\gamma c^{-/-}$
225 mice adoptively transferred with human ILC2 cells (**Fig. 9B**). Moreover, we also observed that the growth
226 and type 2 cytokine production of human ILC2 cells were greatly increased by LPS treatment shown by
227 the FACS cell number and intracellular cytokine staining in these two mouse strains (**Figs. 9C & D**).
228 These data indicate that LPS can function in vivo to initiate human ILC2 cells-mediated eosinophilic
229 lung inflammation.
230
231 **Discussion**
232 In this study, we have discovered a novel function for LPS-TLR4 signaling in activating ILC2 cells. We
233 found that LPS extracted from multiple species of Gram-negative bacteria can potently stimulate human,
234 but not murine ILC2 cells, to proliferate and produce massive amounts of type 2 effector cytokines IL-4,
235 IL-5, and IL-13. This activation of ILC2 cells by the LPS-TLR4 signaling axis does not require the
236 classical IL-33-ST2 pathway but rather requires the NF-kB and JAK pathways. More interestingly, LPS

237 dramatically increased CD40 ligand (CD154) protein level on ILC2 cells to drive the proliferation and
238 antibody production of human B cells. Further, LPS can work in vivo to activate human ILC2 cell in
239 mouse lungs in a humanized mouse model. Mechanistically, RNA-seq data strikingly revealed that LPS
240 upregulated a large set of genes overlapped significantly with those induced by IL-33. To our best
241 knowledge, this is the first time to demonstrate that LPS-TLR4 signaling directly functions in human
242 ILC2 cells to promote their proliferation and production of type 2 effector cytokines independent of the
243 endogenous IL-33-ST2 pathway.
244
245 ILC2 cells are known to be activated by tissues-derived alarmin signals when exposed to environmental
246 allergens. In recent years, accumulating evidence has also suggested that diverse receptors expressed on
247 the surface of ILC2 cells can either enhance or repress their activation and proliferation in response to
248 various non-classical signals, hormones, regulatory cytokines, neuropeptides and lipids (Hurrell et al.,
249 2018). Our findings have identified that TLR4 signaling pathway plays an important role in regulating
250 the survival, proliferation, and the production of type 2 cytokines by human ILC2 cells. Although it was
251 previously shown that human ILC2 cells expressed the mRNA of some TLRs (TLR1, TLR4, and TLR6)
252 and could respond to a mixture of three TLR-ligands (Maggi et al., 2017), it has remained unknown about
253 which TLR pathway actually functions in human ILC2 cells.
254
255 Many previous epidemiological and experimental studies have suggested that endotoxin-TLR4 signaling
256 contributes to the development of type 2 inflammatory reactions (Idzko et al., 2007; Janeway, 1989; Kool
257 et al., 2011; Schuijs et al., 2015; Trompette et al., 2009). However, its underlying cellular and molecular
258 mechanisms remain poorly understood. Natural allergens contain not only allergic proteins, but also
259 various PAMPs derived from bacteria, parasites and viruses, which may stimulate innate immune sensors
260 such as TLRs to participate in the regulation of type 2 inflammatory responses (Locksley, 2010; Palm et
261 al., 2012; Stewart and Thompson, 1996; Van Dyken et al., 2011; Van Dyken et al., 2017; Van Dyken et
262 al., 2014). In the current study we have demonstrated that bacterial endotoxin could directly engage TLR4
263 receptor expressed on the surface of ILC2 cells to robustly activate their proliferation and production of
264 type 2 effector cytokines in culture and in vivo in a humanized mouse model. Besides its classical ligand,
265 LPS, many endogenous ligands such as HMGB1(Tang et al., 2007), hyaluronan (Jiang et al., 2005),
266 OxPAPC (Imai et al., 2008), surfactant protein A (Guillot et al., 2002), S100 proteins (Vogl et al., 1999),
267 HSP72 (Chase et al., 2007; Wheeler et al., 2009) etc. have been reported to act as TLR4 agonists. It has
268 been recently reported that the proteinase-cleavage of fibrinogen could elicits allergic responses through
269 TLR4-mediated pathway (Millien et al., 2013). It would be interesting to evaluate whether those self
270 TLR4 ligands are able to activate human ILC2 cell in future studies.
271
272 ILC2 cells have the ability to communicate with various cell types such as epithelial cells, dendritic cell,
273 Th2 cells and mouse B cells to regulate the tissue-specific immunity (Gurram and Zhu, 2019; Hurrell et
274 al., 2018; Klose and Artis, 2020). In agreement with a recent report showing human ILC2s can express
275 CD154 and stimulate B lymphocytes through IL-25/IL-33 or a mixture of TLR ligands (Maggi et al.,
276 2017), we identified that LPS treatment alone greatly enhanced CD40 ligand (CD154) expression on
277 ILC2 cells and strongly induced three B cell regulatory cytokines IL-4, IL-5, and IL-13, which
278 collectively promote the proliferation and antibody production of human B cells. However, more works
279 are needed in order to understand the underlying mechanisms of antibody-class switching in this context
280 and in vivo significance of these interesting findings.
281

282 In conclusion, our findings support a new mode of activating human ILC2 cells via the LPS-TLR4
283 signaling axis without the involvement of its classical activating pathway mediated by IL-33 receptor,
284 IL1RL1. As to the wide availability of TLR4 ligands, which can originate from either a foreign origin
285 such as bacterial infections or an endogenous source like DAMPs, thus, targeting TLR4 signaling
286 pathway might be developed as a new approach for improving ILC2-mediated type 2 inflammatory
287 conditions.

288 # Material and methods

289 **Mice**

290 *Rag1*$^{-/-}$ mice, *Rag2*$^{-/-}$*γc*$^{-/-}$ (*Rag2*$^{tm1.1Flv}$*Il2rg*$^{tm1.1Flv}$/J, 014593) mice and NSG (NOD.Cg-
291 *Prkdc*^{scid}*Il2rg*^{tm1Wjl}/SzJ, 005557) mice were purchased from the Jackson Laboratory. Mice were bred and
292 maintained under specific pathogen-free conditions in the animal facility according to the experimental
293 protocols approved by the Institutional Animal Care and Use Committee.
294

295 **Regents**

296 The medium used was RPMI 1640 (Sigma) containing 10% FBS (HyClone), 1% penicillin-streptomycin
297 (Gibco), 1x GlutaMAX^{TM}-I (Gibco) and 50 μM 2-Mercaptoethanol (Sigma). PamsCSK4, Poly(I:C),
298 Flagellin, R848 and CpG-A were purchased from InvivoGen. ISR23 was obtained from IDT (Integrated
299 DNA Technologies). LPS from *Escherichia coli* 0127:B8, *Escherichia coli* 055:B5, *Pseudomonas*
300 *aeruginosa* 10 (*P. aeruginosa*), *Salmonella enterica serotype typhimurium* (*S. typhimurium*) were all
301 purchased from Sigma. Recombinant cytokines IL-2, IL-7 and IL-33 (human and mouse) were from
302 PeproTech. TLR4 agonist: CRX-527 (Cat. #tlrl-crx-527) and TLR4 antagonist: LPS-RS Ultrapure (Cat.#
303 tlrl-prslps) were obtained from InvivoGen. Human IL1RL1/ST2 Protein (isoform a, His Tag) (Cat.
304 #13034-H08H) was purchased from Sino Biological. NF-κB inhibitor Bay 11-7802 and JAK inhibitor 1
305 were both from EMD Millipore. PMA and Brefeldin A were purchased from Sigma and BioLegend,
306 respectively.
307

308 **Isolation of ILC2 cells**

309 Human ILC2s were isolated from peripheral blood of healthy donors or umbilical cord blood samples
310 from healthy full-term births in the Department of Obstetrics and Gynecology of UT Health San Antonio.
311 All human samples were used in compliance with UT Health San Antonio Institutional Review Board.
312 Peripheral or Cord Blood Mononuclear Cells (PBMCs or CBMCs) were isolated from diluted umbilical
313 cord blood (1:2) by density gradient centrifugation using density gradient medium, Histopaque® (Sigma
314 Aldrich) and SepMateTM 50 mL tubes (STEMCELL Technologies) (Grievink et al., 2016). Cells were
315 then washed once with dPBS-FBS buffer (dPBS, 3% fetal bovine serum, 1mM EDTA) and resuspended
316 in dPBS-FBS. Cells were stained with antibodies against CD45 and lineage markers (CD3, CD14, CD16,
317 CD19, CD20 and CD56), and ILC2 markers CRTH2, CD127 (all from BioLegend). Human ILC2s were
318 sorted by the BD FACSAria cell sorter as CD45+Lin-CRTH2+CD127+ cells. The purity of sorted ILC2s
319 was determined to be greater than 95%. Sorted human ILC2s were cultured and expanded in medium
320 supplemented with rh-IL-2 and rh-IL-7 (all at 50 ng/mL) in 96-well round plates for 6 days before further
321 experiments.
322

323 Murine Lung ILC2s were isolated from *Rag1*$^{-/-}$ mice treated with rm-IL-33 (250 ng/mouse) for 3
324 consecutive days plus 2 days of resting before processing lung tissues for sorting ILC2 cells with an BD
325 FACSAria cell sorter. The criteria for identifying ILC2 is lacking classical lineage markers (CD3ε, CD4,
326 CD8α, CD11c, FceRIα, NK1.1, CD19, TER119, CD5, F4/80 and Gr-1), but expressing markers of CD45
327 and T1/ST2 (all from BioLegend). The purity of sorted ILC2s should be greater than 95%. Sorted ILC2s
328 were cultured and expanded in medium supplemented with murine IL-2 and IL-7 (all at 10 ng/mL) in 96-
329 well round plates for 6 days before further experiments.
330

331 **Culture and treatment of human and murine ILC2 cells**

332 Sorted human ILC2 were cultured in the medium (200 μl) with or without rh-IL-2, rh-IL-7 and rh-IL-33
333 (all at 50 ng/ml) in 96-well round plates (1,000 cells/well) in a 37℃ incubator with 5% CO_2. Cells were

334 treated with Pam3CSK4, Poly(I:C), LPS, Flagellin, R848, CpG-A and ISR23 (different concentration as
335 indicated) for 3 or 5 days. And the human ILC2 cells were treated with TLR4 agonist or antagonist,
336 human IL1RL1/ST2 Protein (isoform a, His Tag) (added 1 hour prior to the treatment with LPS or IL-
337 33), NF-κB or JAK inhibitor as indicated in figure legends for 5 days. After 3 days treatment, the
338 percentage of IL-5^+IL13^+ cells, the expression of Ki-67 and cell death of ILC2 cells were analyzed by
339 flow cytometry. After 5 days treatment, the number and proliferation of ILC2 cells were analyzed by
340 flow cytometry, and the levels of cytokines (IL-4, IL-5 and IL-13) in the supernatants were measured by
341 ELISA.
342
343 Sorted murine lung ILC2 were cultured and treated with the same TLR ligands in 200 μl media with or
344 without murine IL-2, IL-7 and IL-33 (all at 10ng/ml) in 96-well round plates (1,000 cells/well) in a 37°C
345 incubator with 5% CO_2. The percentage of IL-5^+IL13^+ cells, expression of Ki-67 on murine ILC2 cells
346 were analyzed by flow cytometry 3 days later. The number and proliferation of ILC2 cells were analyzed
347 by flow cytometry 5 days later, and the supernatant were collected for further detecting of IL-5 and IL-
348 13 by ELISA.
349
350 **Flow cytometric analysis**
351 Fc receptors were blocked with 2.4G2 hybridoma supernatant (generated in the lab). For the detection of
352 early-stage apoptotic cells, Annexin V staining was performed according to the protocol (eBioscience).
353 Intranuclear staining of Ki-67 was performed with the True-Nuclear™ Transcription Factor Buffer Set
354 (BioLegend) according to the manufacturer's instructions. For intracellular cytokine staining, human or
355 murine ILC2 cells were cultured and treated as indicated for 3 days, then followed by incubating with
356 Brefeldin A for 3 hours. After surface staining, cells were fixed and permeabilized with BioLegend
357 Cytofix/Perm buffer and further stained intracellularly with anti-human IL-5 and IL-13, or anti-mouse
358 IL-5 and IL-13, respectively. For lung single-cell suspensions, 2 x 10^6 total live nucleated cells were
359 stimulated in 200 μl media with Brefeldin A and PMA (phorbol 12-myristate 13-acetate) (30 ng/mL) at
360 37 °C for 3 hours. After surface staining, cells were fixed and permeabilized and further stained
361 intracellularly with anti-human IL-5 and IL-13. Dead cells were stained with eFluor506 Fixable Viability
362 Dye before fixation and permeabilization and excluded during analysis. For TLR4 and CD14 expression
363 on human ILC2 cells, cells were stained with the surface markers anti-Human TLR4 and anti-Human
364 CD14. For CD154 expression, human ILC2 cells were cultured and stimulated as indicated for 5 days,
365 and followed by staining with anti-Human CD154.
366
367 **Protein quantification in cell culture supernatants**
368 Cytokines (IL-5 and IL-13) in supernatant of human and murine ILC2 cell cultures were analyzed with
369 ELISA kits from Invitrogen. For human cytokine IL-4 in the supernatant of human ILC2 cell cultures
370 were measured by ELISA kit from BioLegend. All final reactions were developed with TMB substrate
371 (Thermo scientific) and stopped by sulfuric acid (0.16M), and the OD at 450 nm was measured.
372
373 **CSFE staining**
374 Human ILC2 cells were stained with 1 μM CSFE (CSFE cell division tracker kit, BioLegend) according
375 to the manufacturer's recommendations. Followed by cultured in the medium with or without rh-IL-2,
376 rh-IL-7, rh-IL-33 (all at 50 ng/ml) or LPS (10 μg/ml) for 3 or 5 days in a 37°C incubator with 5% CO_2.
377 The proliferation of ILC2 cells were analyzed by flow cytometry.
378
379 **Humanized Mice**

380 Purified human ILC2 cells were cultured with rh-IL-2 and rh-IL-7 (all at 50 ng/ml) for 6 days, and then
381 adoptively transferred to NSG mice or *Rag*$^{-/-}$*γc*$^{-/-}$ mice (4 x 10^4 cells/mouse). 4 hours after cell transfer,
382 host mice were challenged with rh-IL-2&7 (all 250 ng/mouse) in absence or presence of LPS (5 μg/mouse)
383 on day 0, 1, 2 as shown in **Fig. 9A**. On day 5, mice were sacrificed, lung was performed and analyzed.
384
385 **FACS analysis of lung**
386 Mice were sacrificed at indicated times and the lung tissues were digested in 8 ml RPMI-1640 containing
387 Liberase (50 μg/ml) and DNase I (1 μg/ml) for about 45 min at 37 °C. Cell suspensions were filtered
388 through 70 μm cell strainers and washed once with RPMI-1640. Human ILC2 cells and mouse
389 eosinophils in lung were labeled with antibodies as indicated, then mixed with counting beads
390 (Spherotech) for further FACS analysis on BD Celesta cell analyzer. Flow cytometry data were analyzed
391 using FlowJo software. The antibodies and reagents for FACS analysis are listed below: SPHERO™
392 AccuCount Fluorescent (Spherotech, Cat.# ACFP-70-5), Anti-Human CD45 APC-Cy7 (HI30,
393 BioLegend), Anti-Human CRTH2 APC (BM16, BioLegend), Anti-Human CD127 PE (A019D5,
394 BioLegend), Anti-Mouse Siglec-F PE (E50-2440, BD Bioscience), Anti-Mouse CD11c PE-Cy7 (N418,
395 TONBO bioscience), Anti-Mouse CD45 PerCP-Cy5.5 (30-F11, BioLegend), Fixable Viability Dye
396 eFluor 506 (Invitrogen).
397
398 **ILC2 and B cells co-culture and Immunoglobulin production**
399 Human naive CD19$^+$ B cells (>95% pure) were purified by negative selection, using the EasySep Human
400 Naive B Cell Enrichment Kit (19254; STEMCELL Technologies), from healthy donor PBMCs,
401 following the manufacturer's instructions. Naïve B cells (2,000/well) were cultured in RPMI medium
402 with rhIL-2&7 (all at 50 ng/ml) or cocultured with ILC2 cells (2,000/well) in the presence of LPS (10
403 μg/ml) in 96-well round plates for 5 days. Supernatants from each well were collected and further
404 evaluated of IgG, IgM, IgA and IgE by a homemade ELISA. Except that 96-well plates were coated with
405 $F(ab')_2$ anti-Ig (H+L) Ab, and captured Igs were detected by biotinylated anti-IgG, -IgA, -IgE and -IgM
406 Abs. Followed by reaction with HRP-labeled streptavidin, development with TMB substrate (Thermo
407 scientific) and stopped by sulfuric acid (0.16M), the OD at 450 nm was measured.
408
409 **Real-Time Quantitative PCR**
410 Human ILC2 cells were treated with or without LPS (10 μg/ml) or rh-IL-33 (50 ng/ml) in 200 μl media
411 with or without rh-IL-2&7 (all 50 ng/ml) for 6 or 16 hours. Total RNA was extracted with TRIzol reagent
412 (Life Technologies) according to the manufacturer's instructions. Reverse transcription and real-time
413 PCR (qPCR) reactions were carried out using iScript cDNA synthesis kit and iQ SYBR Green Supermix
414 (Bio-Rad). qPCR was performed on a Bio-Rad CFX384 Touch™ Real-Time PCR Detection System
415 using the following human primers (Forward and Reverse, 5'→3'): GAPDH
416 (ATGACATCAAGAAGGTGGTG; CATACCAGGAAATGAGCTTG), IL-4
417 (ACTTTGAACAGCCTCACAGAG; TTGGAGGCAGCAAAGATGTC), IL-5
418 (AGCTGCCTACGTGTATGCCA; CAGGAACAGGAATCCTCAGA), IL-13
419 (TGAGGAGCTGGTCAACATCA; CAGGTTGATGCTCCATACCAT), TNFα
420 (CCTGGTATGAGCCCATCTATCTG; TAGTCGGGCCGATTGATCTC).
421
422 **RNA isolation, RNA-Seq and Bioinformatics**
423 Purified human ILC2 cells (4x10^4) were cultured and stimulated with LPS (10 μg/ml) or recombinant
424 human IL-33 protein (rh-IL-33) (50 ng/ml) in the presence with rh-IL-2&7 (all at 50 ng/ml) for 6 hours.
425 Total RNA was extracted with RNeasy Mini Kit (Qiagen) according to the manufacturer's instructions.

After the quality of RNA samples was verified with an Agilent Bioanalyzer 2100 (Agilent), RNA was further processed using an Illumina TruSeq RNA sample prep kit v2 (Illumina). Clusters were generated using TruSeq Single-Read Cluster Gen. Kit v3-cBot-HS on an Illumina cBot Cluster Generation Station. After the quality control procedures, individual RNA-Seq libraries were pooled based on their respective 6 bp index portion of the TruSeq adapters and sequenced at 50 bp/sequence using an Illumina HiSeq 3000 sequencer. Resulting reads were checked by assurance (QA) pipeline and initial genome alignment (Alignment). After sequencing, demultiplexing with CASAVA was employed to generate a Fastq file for each sample. All sequencing reads were aligned with the (GRCh38/hg38) reference genome using HISAT2 default settings, yielding Bam files, duplicated reads were discarded by using Picard, then were processed using HTSeq-count to obtain counts for each gene. RNA expression levels were determined using GENCODE annotation. Differential expression analysis was performed using the Deseq2 package in R post-normalization based on a Benjamini-Hochberg false discovery rate (FDR)-corrected threshold for statistical significance of padj <0.05 or raw p value <0.01. Transcript read counts were transformed to $\ln(x+1)$ used to generate heatmaps in Clustvis. Volcano plots depicting log2-FoldChange and raw or adjusted p values were generated in R. Venn diagram were generated by use the VennDiagram package in R.

To investigate biological pathways, DEGs (Differential Expression Genes) were manually curated and compared to multiple public databases, including Gene Ontology (GO) and Kyoto Encyclopedia of Genes and Genomes (KEGG), for enrichment analysis. For gene set enrichment analysis (GSEA), IL-33 upregulated gene set was identified from our RNASeq data comparing the sample rh-IL-33 in the presence of rh-IL-2&7 with the sample only has rh-IL-2&7 stimulation by using the threshold for statistical significance raw p value <0.01 and log2-FoldChange >1. Samples with or without LPS in the presence of rh-IL-2&7 were directly compared to this gene set to identify statistically significant concordance in the expression using the gene set enrichment analysis (GSEA) algorithm.

Statistical analysis

The statistical analysis was done using software GraphPad Prism 6. For comparison of two groups, P values were determined by unpaired two-tailed Student's t test. For comparison of more than two groups, Two-Way ANOVA was performed. P values are indicated on plots and in figure legends. P value<0.05 was considered statistically significant. (P value ≥ 0.05 was not considered statistically significant [N.S.]. * $p < 0.05$, ** $p < 0.01$, *** $p < 0.001$, **** $p < 0.0001$).

Acknowledgements

We thank Ms. Karla Gorena, Mr. Sebastian Montagnino for technical assistance in flow cytometry and FACS sorting. We thank Drs. Zhao Lai, Yi Zou, and Yidong Chen for RNA-seq analysis and informatics assistance. L.S. is supported by the China Scholarship Council and Hunan Provincial Innovation Foundation for Postgraduate (CX201713068). H.H.A. is supported by the Department of Clinical Laboratory Sciences, College of Applied Medical Sciences, Jouf University, Sakaka, Saudi Arabia. X.-D.L. is supported by the UT Health San Antonio School of Medicine Startup Fund and the Max and Minnei Voelcker Fund.

Author contributions

L.S. and H.H.A. performed most experiments; L.S., H.H.A., J.W., D.P.C., Y.X., H.Z., Z.X., Y.S., N.X., X.Z., Y.L. and X.-D.L. analyzed data; L.S., H.H.A., Y.L. and X.-D.L. planned, designed research. L.S.,

Y.L. and X.-D.L. wrote the manuscript; All authors discussed the results and participated in writing and commenting on the manuscript.

Competing interests: The authors declare no conflict of interest.

477 **REFERENCES**

478 Akira, S., S. Uematsu, and O. Takeuchi. 2006. Pathogen recognition and innate immunity. *Cell*
479 124:783-801.
480 Artis, D., and H. Spits. 2015. The biology of innate lymphoid cells. *Nature* 517:293-301.
481 Barlow, J.L., and A.N.J. McKenzie. 2019. Innate Lymphoid Cells of the Lung. *Annu Rev Physiol*
482 81:429-452.
483 Bourke, E., D. Bosisio, J. Golay, N. Polentarutti, and A. Mantovani. 2003. The toll-like receptor
484 repertoire of human B lymphocytes: inducible and selective expression of TLR9 and TLR10 in
485 normal and transformed cells. *Blood* 102:956-963.
486 Brubaker, S.W., K.S. Bonham, I. Zanoni, and J.C. Kagan. 2015. Innate immune pattern recognition: a
487 cell biological perspective. *Annu Rev Immunol* 33:257-290.
488 Cayrol, C., and J.P. Girard. 2018. Interleukin-33 (IL-33): A nuclear cytokine from the IL-1 family.
489 *Immunol Rev* 281:154-168.
490 Chase, M.A., D.S. Wheeler, K.M. Lierl, V.S. Hughes, H.R. Wong, and K. Page. 2007. Hsp72 induces
491 inflammation and regulates cytokine production in airway epithelium through a TLR4- and NF-
492 kappaB-dependent mechanism. *J Immunol* 179:6318-6324.
493 Coats, S.R., T.T. Pham, B.W. Bainbridge, R.A. Reife, and R.P. Darveau. 2005. MD-2 mediates the
494 ability of tetra-acylated and penta-acylated lipopolysaccharides to antagonize Escherichia coli
495 lipopolysaccharide at the TLR4 signaling complex. *J Immunol* 175:4490-4498.
496 Crellin, N.K., S. Trifari, C.D. Kaplan, N. Satoh-Takayama, J.P. Di Santo, and H. Spits. 2010.
497 Regulation of cytokine secretion in human CD127(+) LTi-like innate lymphoid cells by Toll-
498 like receptor 2. *Immunity* 33:752-764.
499 Deckers, J., K. De Bosscher, B.N. Lambrecht, and H. Hammad. 2017. Interplay between barrier
500 epithelial cells and dendritic cells in allergic sensitization through the lung and the skin.
501 *Immunol Rev* 278:131-144.
502 Defrance, T., P. Carayon, G. Billian, J.C. Guillemot, A. Minty, D. Caput, and P. Ferrara. 1994.
503 Interleukin 13 is a B cell stimulating factor. *J Exp Med* 179:135-143.
504 Drake, L.Y., K. Iijima, K. Bartemes, and H. Kita. 2016. Group 2 Innate Lymphoid Cells Promote an
505 Early Antibody Response to a Respiratory Antigen in Mice. *J Immunol* 197:1335-1342.
506 Eberl, G., M. Colonna, J.P. Di Santo, and A.N. McKenzie. 2015. Innate lymphoid cells. Innate
507 lymphoid cells: a new paradigm in immunology. *Science* 348:aaa6566.
508 Eisenbarth, S.C., D.A. Piggott, J.W. Huleatt, I. Visintin, C.A. Herrick, and K. Bottomly. 2002.
509 Lipopolysaccharide-enhanced, toll-like receptor 4-dependent T helper cell type 2 responses to
510 inhaled antigen. *J Exp Med* 196:1645-1651.
511 Ganley-Leal, L.M., Y. Liang, M. Jagannathan-Bogdan, F.A. Farraye, and B.S. Nikolajczyk. 2010.
512 Differential regulation of TLR4 expression in human B cells and monocytes. *Mol Immunol*
513 48:82-88.
514 Grievink, H.W., T. Luisman, C. Kluft, M. Moerland, and K.E. Malone. 2016. Comparison of Three
515 Isolation Techniques for Human Peripheral Blood Mononuclear Cells: Cell Recovery and
516 Viability, Population Composition, and Cell Functionality. *Biopreserv Biobank* 14:410-415.
517 Guillot, L., V. Balloy, F.X. McCormack, D.T. Golenbock, M. Chignard, and M. Si-Tahar. 2002.
518 Cutting edge: the immunostimulatory activity of the lung surfactant protein-A involves Toll-like
519 receptor 4. *J Immunol* 168:5989-5992.
520 Gurram, R.K., and J. Zhu. 2019. Orchestration between ILC2s and Th2 cells in shaping type 2 immune
521 responses. *Cell Mol Immunol* 16:225-235.

522 Halim, T.Y., Y.Y. Hwang, S.T. Scanlon, H. Zaghouani, N. Garbi, P.G. Fallon, and A.N. McKenzie.
523 2016. Group 2 innate lymphoid cells license dendritic cells to potentiate memory TH2 cell
524 responses. *Nat Immunol* 17:57-64.
525 Hammad, H., M. Chieppa, F. Perros, M.A. Willart, R.N. Germain, and B.N. Lambrecht. 2009. House
526 dust mite allergen induces asthma via Toll-like receptor 4 triggering of airway structural cells.
527 *Nat Med* 15:410-416.
528 Hammad, H., and B.N. Lambrecht. 2015. Barrier Epithelial Cells and the Control of Type 2 Immunity.
529 *Immunity* 43:29-40.
530 Hurrell, B.P., L. Galle-Treger, P.S. Jahani, E. Howard, D.G. Helou, H. Banie, P. Soroosh, and O.
531 Akbari. 2019. TNFR2 Signaling Enhances ILC2 Survival, Function, and Induction of Airway
532 Hyperreactivity. *Cell Rep* 29:4509-4524 e4505.
533 Hurrell, B.P., P. Shafiei Jahani, and O. Akbari. 2018. Social Networking of Group Two Innate
534 Lymphoid Cells in Allergy and Asthma. *Front Immunol* 9:2694.
535 Idzko, M., H. Hammad, M. van Nimwegen, M. Kool, M.A. Willart, F. Muskens, H.C. Hoogsteden, W.
536 Luttmann, D. Ferrari, F. Di Virgilio, J.C. Virchow, Jr., and B.N. Lambrecht. 2007. Extracellular
537 ATP triggers and maintains asthmatic airway inflammation by activating dendritic cells. *Nat*
538 *Med* 13:913-919.
539 Imai, Y., K. Kuba, G.G. Neely, R. Yaghubian-Malhami, T. Perkmann, G. van Loo, M. Ermolaeva, R.
540 Veldhuizen, Y.H. Leung, H. Wang, H. Liu, Y. Sun, M. Pasparakis, M. Kopf, C. Mech, S.
541 Bavari, J.S. Peiris, A.S. Slutsky, S. Akira, M. Hultqvist, R. Holmdahl, J. Nicholls, C. Jiang, C.J.
542 Binder, and J.M. Penninger. 2008. Identification of oxidative stress and Toll-like receptor 4
543 signaling as a key pathway of acute lung injury. *Cell* 133:235-249.
544 Ingley, E., R.L. Cutler, M.C. Fung, C.J. Sanderson, and I.G. Young. 1991. Production and purification
545 of recombinant human interleukin-5 from yeast and baculovirus expression systems. *Eur J*
546 *Biochem* 196:623-629.
547 Ishii, T., M. Muroi, K. Horiguchi, K.I. Tanamoto, T. Nagase, and N. Yamashita. 2019. Activation
548 through toll-like receptor 2 on group 2 innate lymphoid cells can induce asthmatic
549 characteristics. *Clin Exp Allergy* 49:1624-1632.
550 Jackson, K.D., L.D. Howie, and L.J. Akinbami. 2013. Trends in allergic conditions among children:
551 United States, 1997-2011. *NCHS Data Brief* 1-8.
552 Janeway, C.A., Jr. 1989. Approaching the asymptote? Evolution and revolution in immunology. *Cold*
553 *Spring Harb Symp Quant Biol* 54 Pt 1:1-13.
554 Jiang, D., J. Liang, J. Fan, S. Yu, S. Chen, Y. Luo, G.D. Prestwich, M.M. Mascarenhas, H.G. Garg,
555 D.A. Quinn, R.J. Homer, D.R. Goldstein, R. Bucala, P.J. Lee, R. Medzhitov, and P.W. Noble.
556 2005. Regulation of lung injury and repair by Toll-like receptors and hyaluronan. *Nat Med*
557 11:1173-1179.
558 Kaisho, T., and S. Akira. 2006. Toll-like receptor function and signaling. *J Allergy Clin Immunol*
559 117:979-987; quiz 988.
560 Kay, A.B. 2001a. Allergy and allergic diseases. First of two parts. *N Engl J Med* 344:30-37.
561 Kay, A.B. 2001b. Allergy and allergic diseases. Second of two parts. *N Engl J Med* 344:109-113.
562 Klose, C.S.N., and D. Artis. 2020. Innate lymphoid cells control signaling circuits to regulate tissue-
563 specific immunity. *Cell Res* 30:475-491.
564 Kool, M., M.A. Willart, M. van Nimwegen, I. Bergen, P. Pouliot, J.C. Virchow, N. Rogers, F. Osorio,
565 C. Reis e Sousa, H. Hammad, and B.N. Lambrecht. 2011. An unexpected role for uric acid as an
566 inducer of T helper 2 cell immunity to inhaled antigens and inflammatory mediator of allergic
567 asthma. *Immunity* 34:527-540.

568 Kubo, M. 2017. Innate and adaptive type 2 immunity in lung allergic inflammation. *Immunol Rev*
569 278:162-172.
570 Li, X.D., and Z.J. Chen. 2012. Sequence specific detection of bacterial 23S ribosomal RNA by TLR13.
571 *Elife* 1:e00102.
572 Liew, F.Y., J.P. Girard, and H.R. Turnquist. 2016. Interleukin-33 in health and disease. *Nat Rev*
573 *Immunol* 16:676-689.
574 Locksley, R.M. 2010. Asthma and allergic inflammation. *Cell* 140:777-783.
575 Maazi, H., H. Banie, G.R. Aleman Muench, N. Patel, B. Wang, I. Sankaranarayanan, V. Bhargava, T.
576 Sato, G. Lewis, M. Cesaroni, J. Karras, A. Das, P. Soroosh, and O. Akbari. 2018. Activated
577 plasmacytoid dendritic cells regulate type 2 innate lymphoid cell-mediated airway
578 hyperreactivity. *J Allergy Clin Immunol* 141:893-905 e896.
579 Maggi, L., G. Montaini, A. Mazzoni, B. Rossettini, M. Capone, M.C. Rossi, V. Santarlasci, F. Liotta,
580 O. Rossi, O. Gallo, R. De Palma, E. Maggi, L. Cosmi, S. Romagnani, and F. Annunziato. 2017.
581 Human circulating group 2 innate lymphoid cells can express CD154 and promote IgE
582 production. *J Allergy Clin Immunol* 139:964-976 e964.
583 Man, S.M., R. Karki, and T.D. Kanneganti. 2016. AIM2 inflammasome in infection, cancer, and
584 autoimmunity: Role in DNA sensing, inflammation, and innate immunity. *Eur J Immunol*
585 46:269-280.
586 McAlees, J.W., G.S. Whitehead, I.T. Harley, M. Cappelletti, C.L. Rewerts, A.M. Holdcroft, S.
587 Divanovic, M. Wills-Karp, F.D. Finkelman, C.L. Karp, and D.N. Cook. 2015. Distinct Tlr4-
588 expressing cell compartments control neutrophilic and eosinophilic airway inflammation.
589 *Mucosal Immunol* 8:863-873.
590 Millien, V.O., W. Lu, J. Shaw, X. Yuan, G. Mak, L. Roberts, L.Z. Song, J.M. Knight, C.J. Creighton,
591 A. Luong, F. Kheradmand, and D.B. Corry. 2013. Cleavage of fibrinogen by proteinases elicits
592 allergic responses through Toll-like receptor 4. *Science* 341:792-796.
593 Moens, L., and S.G. Tangye. 2014. Cytokine-Mediated Regulation of Plasma Cell Generation: IL-21
594 Takes Center Stage. *Front Immunol* 5:65.
595 Molofsky, A.B., A.K. Savage, and R.M. Locksley. 2015. Interleukin-33 in Tissue Homeostasis, Injury,
596 and Inflammation. *Immunity* 42:1005-1019.
597 Moon, B.G., S. Takaki, K. Miyake, and K. Takatsu. 2004. The role of IL-5 for mature B-1 cells in
598 homeostatic proliferation, cell survival, and Ig production. *J Immunol* 172:6020-6029.
599 Palm, N.W., R.K. Rosenstein, and R. Medzhitov. 2012. Allergic host defences. *Nature* 484:465-472.
600 Roach, J.C., G. Glusman, L. Rowen, A. Kaur, M.K. Purcell, K.D. Smith, L.E. Hood, and A. Aderem.
601 2005. The evolution of vertebrate Toll-like receptors. *Proc Natl Acad Sci U S A* 102:9577-9582.
602 Sabatel, C., C. Radermecker, L. Fievez, G. Paulissen, S. Chakarov, C. Fernandes, S. Olivier, M.
603 Toussaint, D. Pirottin, X. Xiao, P. Quatresooz, J.C. Sirard, D. Cataldo, L. Gillet, H. Bouabe,
604 C.J. Desmet, F. Ginhoux, T. Marichal, and F. Bureau. 2017. Exposure to Bacterial CpG DNA
605 Protects from Airway Allergic Inflammation by Expanding Regulatory Lung Interstitial
606 Macrophages. *Immunity* 46:457-473.
607 Schuijs, M.J., M.A. Willart, K. Vergote, D. Gras, K. Deswarte, M.J. Ege, F.B. Madeira, R. Beyaert, G.
608 van Loo, F. Bracher, E. von Mutius, P. Chanez, B.N. Lambrecht, and H. Hammad. 2015. Farm
609 dust and endotoxin protect against allergy through A20 induction in lung epithelial cells.
610 *Science* 349:1106-1110.
611 Stewart, G.A., and P.J. Thompson. 1996. The biochemistry of common aeroallergens. *Clin Exp Allergy*
612 26:1020-1044.

613 Stover, A.G., J. Da Silva Correia, J.T. Evans, C.W. Cluff, M.W. Elliott, E.W. Jeffery, D.A. Johnson,
614 M.J. Lacy, J.R. Baldridge, P. Probst, R.J. Ulevitch, D.H. Persing, and R.M. Hershberg. 2004.
615 Structure-activity relationship of synthetic toll-like receptor 4 agonists. *J Biol Chem* 279:4440-
616 4449.
617 Tang, A.H., G.J. Brunn, M. Cascalho, and J.L. Platt. 2007. Pivotal advance: endogenous pathway to
618 SIRS, sepsis, and related conditions. *J Leukoc Biol* 82:282-285.
619 Tavernier, J., S. Cornelis, R. Devos, Y. Guisez, G. Plaetinck, and J. Van der Heyden. 1995.
620 Structure/function analysis of human interleukin 5 and its receptor. *Agents Actions Suppl* 46:23-
621 34.
622 Thio, C.L., A.C. Lai, P.Y. Chi, G. Webster, and Y.J. Chang. 2019. Toll-like receptor 9-dependent
623 interferon production prevents group 2 innate lymphoid cell-driven airway hyperreactivity. *J*
624 *Allergy Clin Immunol*
625 Trompette, A., S. Divanovic, A. Visintin, C. Blanchard, R.S. Hegde, R. Madan, P.S. Thorne, M. Wills-
626 Karp, T.L. Gioannini, J.P. Weiss, and C.L. Karp. 2009. Allergenicity resulting from functional
627 mimicry of a Toll-like receptor complex protein. *Nature* 457:585-588.
628 Van Dyken, S.J., D. Garcia, P. Porter, X. Huang, P.J. Quinlan, P.D. Blanc, D.B. Corry, and R.M.
629 Locksley. 2011. Fungal chitin from asthma-associated home environments induces eosinophilic
630 lung infiltration. *J Immunol* 187:2261-2267.
631 Van Dyken, S.J., H.E. Liang, R.P. Naikawadi, P.G. Woodruff, P.J. Wolters, D.J. Erle, and R.M.
632 Locksley. 2017. Spontaneous Chitin Accumulation in Airways and Age-Related Fibrotic Lung
633 Disease. *Cell* 169:497-509 e413.
634 Van Dyken, S.J., A. Mohapatra, J.C. Nussbaum, A.B. Molofsky, E.E. Thornton, S.F. Ziegler, A.N.
635 McKenzie, M.F. Krummel, H.E. Liang, and R.M. Locksley. 2014. Chitin activates parallel
636 immune modules that direct distinct inflammatory responses via innate lymphoid type 2 and
637 gammadelta T cells. *Immunity* 40:414-424.
638 Vivier, E., D. Artis, M. Colonna, A. Diefenbach, J.P. Di Santo, G. Eberl, S. Koyasu, R.M. Locksley,
639 A.N.J. McKenzie, R.E. Mebius, F. Powrie, and H. Spits. 2018. Innate Lymphoid Cells: 10
640 Years On. *Cell* 174:1054-1066.
641 Vogl, T., C. Propper, M. Hartmann, A. Strey, K. Strupat, C. van den Bos, C. Sorg, and J. Roth. 1999.
642 S100A12 is expressed exclusively by granulocytes and acts independently from MRP8 and
643 MRP14. *J Biol Chem* 274:25291-25296.
644 Wheeler, D.S., M.A. Chase, A.P. Senft, S.E. Poynter, H.R. Wong, and K. Page. 2009. Extracellular
645 Hsp72, an endogenous DAMP, is released by virally infected airway epithelial cells and
646 activates neutrophils via Toll-like receptor (TLR)-4. *Respir Res* 10:31.
647 Wu, J., and Z.J. Chen. 2014. Innate immune sensing and signaling of cytosolic nucleic acids. *Annu Rev*
648 *Immunol* 32:461-488.
649

Figure 1

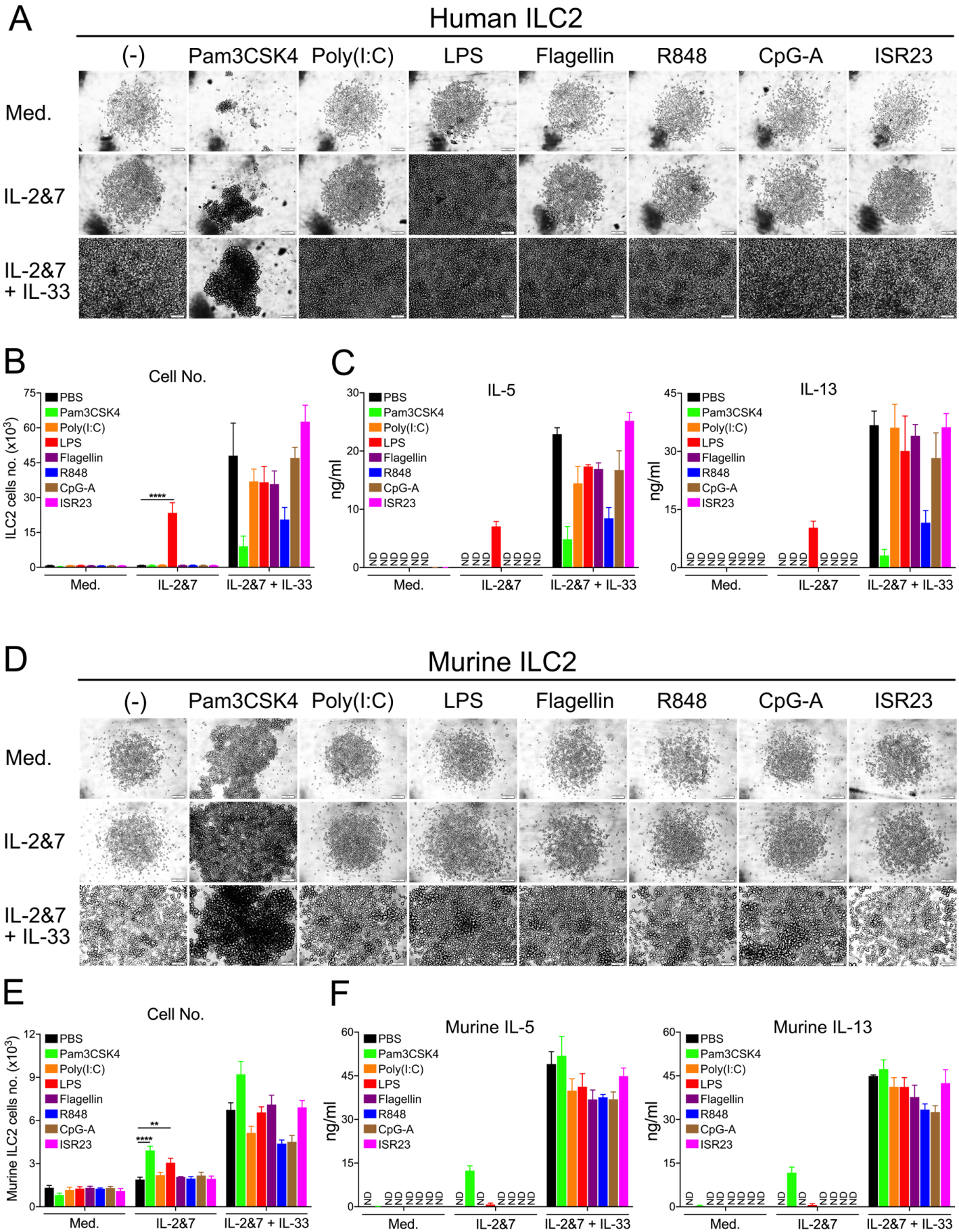
A
Human ILC2
(-)
Pam3CSK4
Poly(I:C)
LPS
Flagellin
R848
CpG-A
ISR23
Med.
IL-2&7
IL-2&7 + IL-33
B
Cell No.
ILC2 cells no. (x10³)
PBS
Pam3CSK4
Poly(I:C)
LPS
Flagellin
R848
CpG-A
ISR23
****
Med.
IL-2&7
IL-2&7 + IL-33
C
IL-5
IL-13
ng/ml
ND
D
Murine ILC2
E
Cell No.
Murine ILC2 cells no. (x10³)
**
F
Murine IL-5
Murine IL-13

Figure 1. LPS strongly stimulated the growth and cytokine production of human, but not murine ILC2. A. Light microscopic images showing the growth of ILC2 cells. FACS sorted human ILC2 cells were treated with various TLRs as indicated in a 96-well round-bottom plate for 5 days. Each image represented one well in which 1,000 cells were initially seeded. Scale bar, 100 μm. **B.** FACS showing the number of human ILC2 cells treated with various TLRs as indicated. **C**. ELISA measuring the production of IL-5 and IL-13 by human ILC2 cells treated with various TLR ligands as indicated. **D.** Light microscopic images showing the growth of ILC2 cells. FACS sorted murine ILC2 cells were treated with various TLR ligands as indicated in a 96-well round-bottom plate for 5 days. Each image represented one well in which 1,000 cells were initially seeded. Scale bar, 100 μm. **E.** FACS showing the number of murine ILC2 cells treated with various TLRs as indicated. **F**. ELISA measuring the production of IL-5 and IL-13 by murine ILC2 cells treated with various TLRs as indicated. (P value <0.05 was considered statistically significant, two-way ANOVA, ** $p < 0.01$, **** $p < 0.0001$).

Figure 2

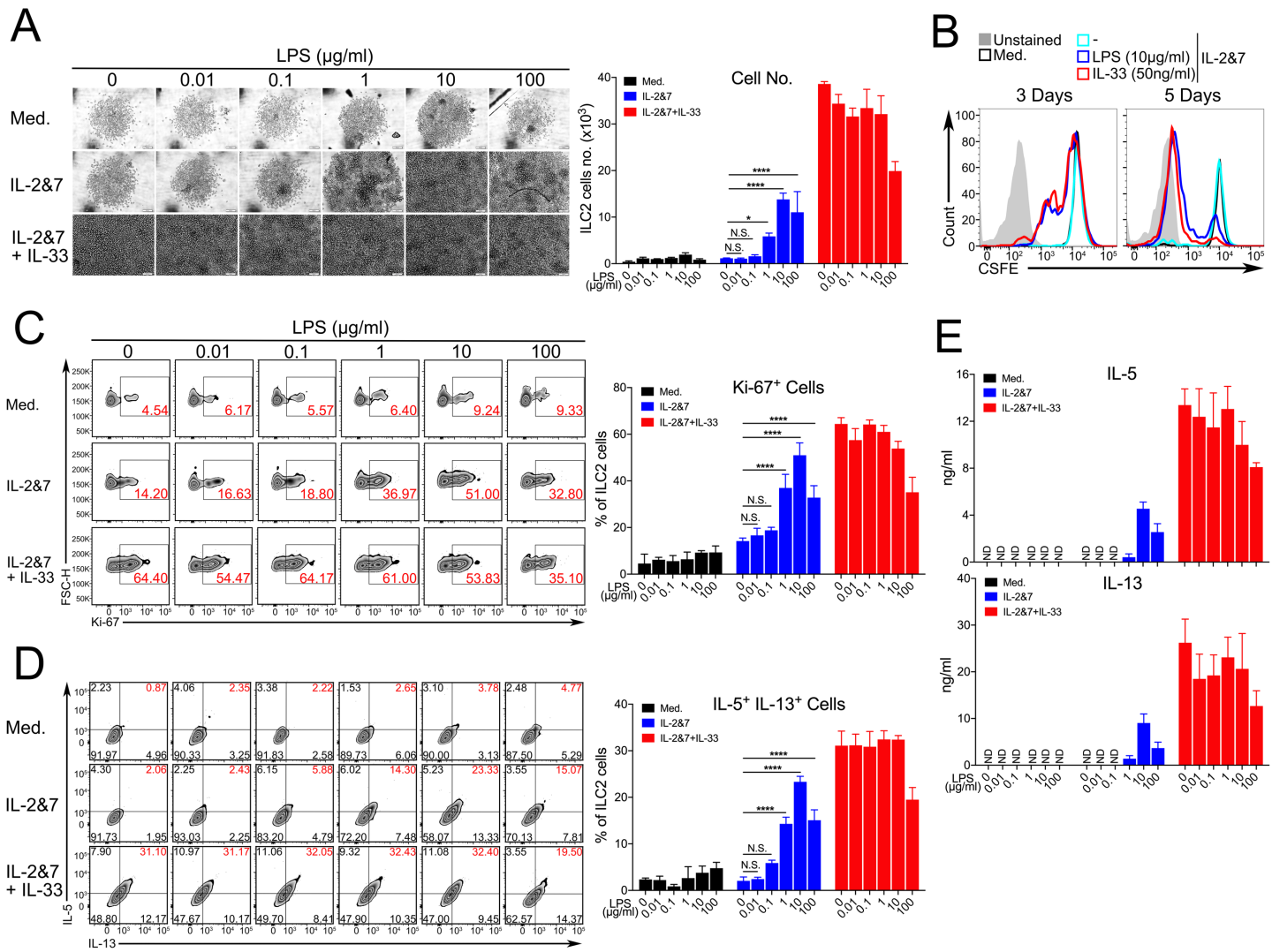

Figure 2. LPS stimulated human ILC2 cells in a dose-dependent manner. A. Light microscopic images showing the growth of ILC2 cells. FACS sorted human ILC2 cells were treated with the increased dose of LPS as indicated. Each image represented one well in which 1,000 cells were initially seeded in a 96-well round-bottom plate. Scale bar, 100 μm (left). FACS showing the number of LPS-treated human ILC2 cells (right). **B.** CSFE labelling for tacking the proliferation of human ILC2 cells treated with LPS or IL-33 for 3 or 5 days. **C.** The proliferation of LPS-treated human ILC2 cells were analyzed with Ki-67 staining. The representative FACS gating images and quantification of Ki-67 positive cells were shown. The result is a representative of two independent experiments. **D**. The percentage of IL5+IL13+-double positive human ILC2 cells treated with the increased dose of LPS were analyzed by the intracellular staining. (P value <0.05 was considered statistically significant, two-way ANOVA, **** $p < 0.0001$). **E.** ELISA measuring the production of IL-5 and IL-13 by human ILC2 cells treated with the increased dose of LPS.

Figure 3

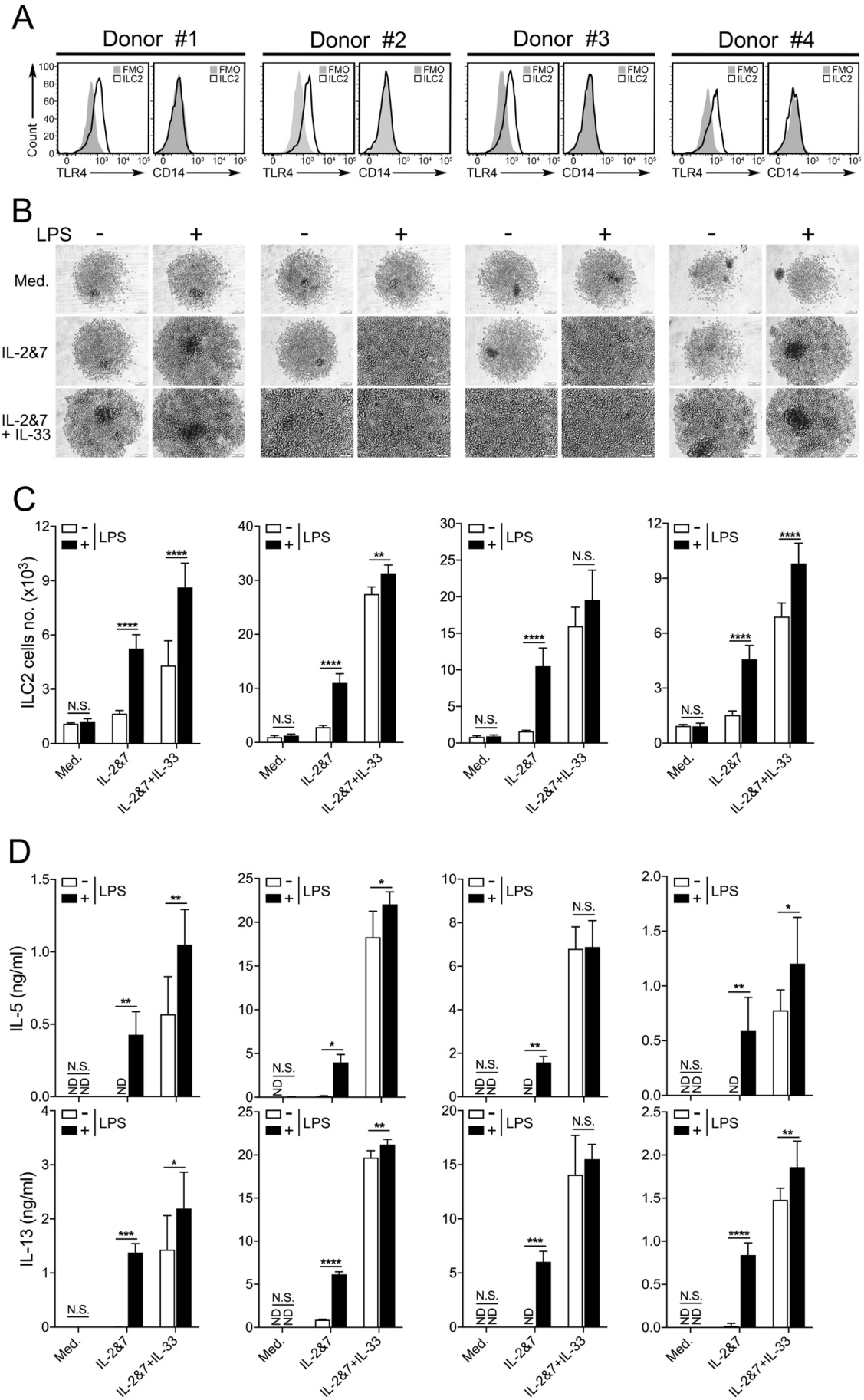
A
Donor #1
Donor #2
Donor #3
Donor #4
FMO
ILC2
Count
TLR4
CD14
B
LPS
-
+
Med.
IL-2&7
IL-2&7
+ IL-33
C
ILC2 cells no. (x10³)
N.S.
****
**
Med.
IL-2&7
IL-2&7+IL-33
D
IL-5 (ng/ml)
IL-13 (ng/ml)
ND
*
***

Figure 3. TLR4 expression and the LPS responsiveness of human ILC2 cells from four healthy donors. **A.** FACS staining of TLR4 or CD14 proteins on the surface of human ILC2 cells. FMO (Fluorescence Minus One control). **B.** Light microscopic images showing the growth of ILC2 cells derived from 4 individual donors were activated by LPS or IL-33. Each image represented one well in which 1,000 cells were initially seeded. Scale bar, 100 μm. **C.** FACS showing the number of human ILC2 cells derived from 4 individual donors were activated by LPS. **D.** ELISA measuring the production of IL-5 and IL-13 by human ILC2 cells treated with LPS. (P value≥0.05 was considered statistically insignificant, N.S., two-way ANOVA, * $p < 0.05$, ** $p < 0.01$, *** $p < 0.001$, **** $p < 0.0001$).

Figure 4

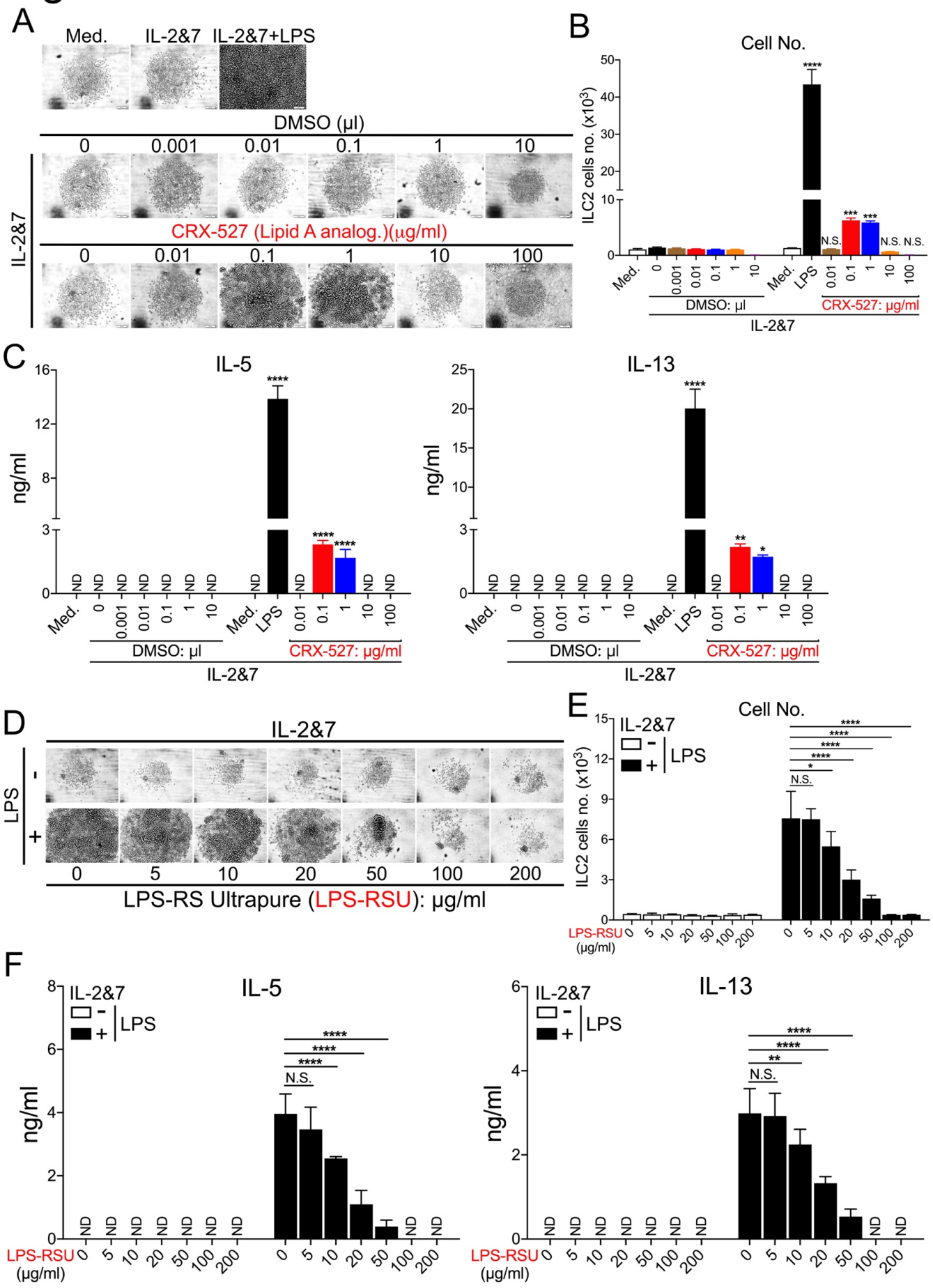
A
Med.
IL-2&7
IL-2&7+LPS
DMSO (µl)
0
0.001
0.01
0.1
1
10
IL-2&7
CRX-527 (Lipid A analog.)(µg/ml)
0
0.01
0.1
1
10
100
B
Cell No.
ILC2 cells no. (x10³)
Med.
LPS
DMSO: µl
CRX-527: µg/ml
IL-2&7
N.S.
C
IL-5
IL-13
ng/ml
ND
D
IL-2&7
LPS
-
+
0
5
10
20
50
100
200
LPS-RS Ultrapure (LPS-RSU): µg/ml
E
Cell No.
IL-2&7
LPS
ILC2 cells no. (x10³)
LPS-RSU (µg/ml)
F
IL-5
IL-13
ng/ml
LPS-RSU (µg/ml)

Figure 4. Stimulation and suppression of human ILC2 cells by the synthetic agonist or antagonist of LPS. A. Light microscopic images showing the growth of ILC2 cells treated with CRX-527, lipid A analog or its solvent DMSO. FACS sorted human ILC2 cells were treated with the increased dose of CRX-527 as indicated. Each image represented one well in which 1,000 cells were initially seeded. Scale bar, 100 µm. **B.** FACS showing the number of human ILC2 cells treated with either CRX-527 or DMSO. **C.** ELISA measuring the production of IL-5 and IL-13 by human ILC2 cells treated with either CRX527 or DMSO. **D.** Light microscopic images showed that the LPS-stimulated growth of ILC2 cells were inhibited by the increased dose of a specific TLR4 antagonist, LPS-RS. Each image represented one well in which 1,000 cells were initially seeded. Scale bar, 100 µm. **E.** FACS showing the number of human ILC2 cells treated with LPS-RS. **F.** ELISA measuring the production of IL-5 and IL-13 by human ILC2 cells treated with the increased doses of LPS-RS. (* P value <0.05 was considered statistically significant, unpaired t-test, ** $p < 0.01$, *** $p < 0.001$, **** $p < 0.0001$).

Figure 5

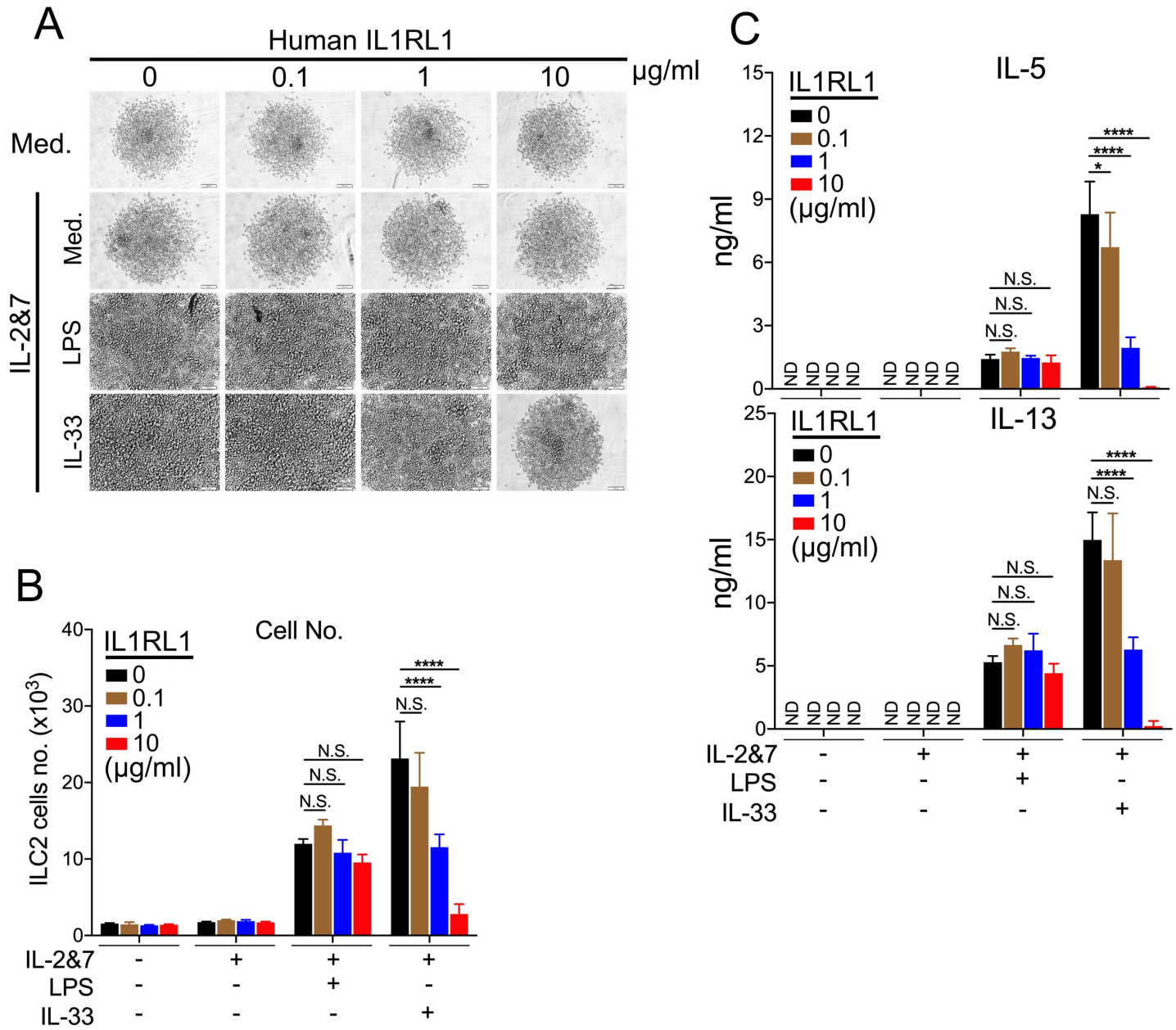

Figure 5. LPS-activated human ILC2 cells are insensitive to the blocking effects of recombinant protein IL1RL1, the IL-33 receptor. A. Light microscopic images showing the growth of ILC2 cells treated with the increased dose of recombinant protein IL1RL1. FACS sorted human ILC2 cells were activated with either LPS or IL-33 as indicated. Each image represented one well in which 1,000 cells were initially seeded. Scale bar, 100μm. **B.** FACS showing the number of human ILC2 cells treated with the increased dose of recombinant protein IL1RL1. **C.** ELISA measuring the production of IL-5 and IL-13 by human ILC2 cells treated with the increased dose of recombinant protein IL1RL1. (P value <0.05 was considered statistically significant, two-way ANOVA, **** $p < 0.0001$).

Figure 6

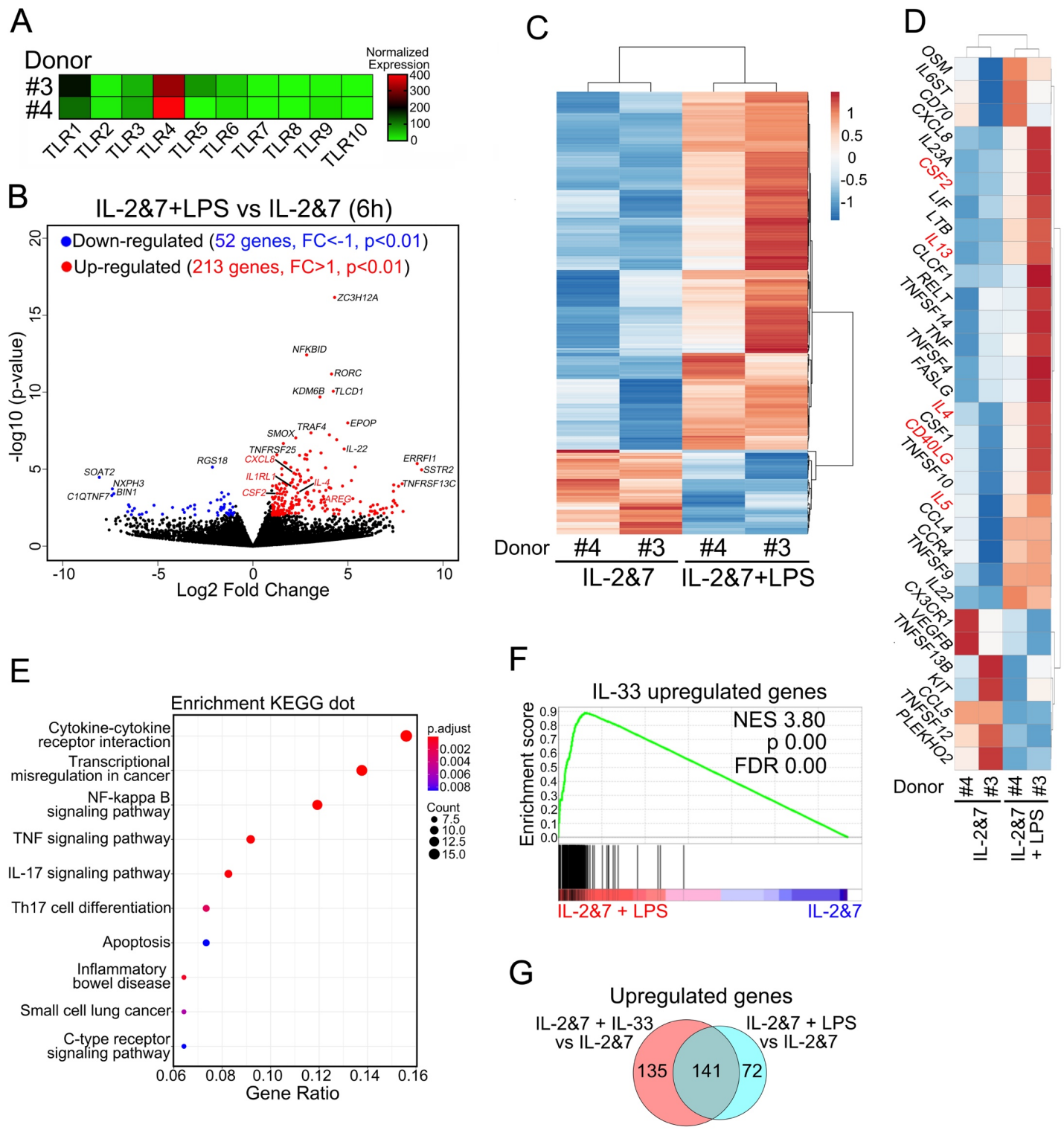
A
Donor
#3
#4
TLR1
TLR2
TLR3
TLR4
TLR5
TLR6
TLR7
TLR8
TLR9
TLR10
Normalized Expression
400
300
200
100
0
B
IL-2&7+LPS vs IL-2&7 (6h)
Down-regulated (52 genes, FC<-1, p<0.01)
Up-regulated (213 genes, FC>1, p<0.01)
-log10 (p-value)
Log2 Fold Change
ZC3H12A
NFKBID
RORC
KDM6B
TLCD1
EPOP
TRAF4
SMOX
TNFRSF25
IL-22
CXCL8
RGS18
ERRFI1
SSTR2
SOAT2
NXPH3
BIN1
C1QTNF7
IL1RL1
IL-4
TNFRSF13C
CSF2
AREG
C
Donor
#4
#3
#4
#3
IL-2&7
IL-2&7+LPS
1
0.5
0
-0.5
-1
D
OSM
IL6ST
CD70
CXCL8
IL23A
CSF2
LIF
LTB
IL13
CLCF1
RELT
TNFSF14
TNF
TNFSF4
FASLG
IL4
CSF1
CD40LG
TNFSF10
IL5
CCL4
CCR4
TNFSF9
IL22
CX3CR1
VEGFB
TNFSF13B
KIT
CCL5
TNFSF12
PLEKHO2
Donor
#4
#3
#4
#3
IL-2&7
IL-2&7 + LPS
E
Enrichment KEGG dot
Cytokine-cytokine receptor interaction
Transcriptional misregulation in cancer
NF-kappa B signaling pathway
TNF signaling pathway
IL-17 signaling pathway
Th17 cell differentiation
Apoptosis
Inflammatory bowel disease
Small cell lung cancer
C-type receptor signaling pathway
Gene Ratio
p.adjust
0.002
0.004
0.006
0.008
Count
7.5
10.0
12.5
15.0
F
IL-33 upregulated genes
Enrichment score
NES 3.80
p 0.00
FDR 0.00
IL-2&7 + LPS
IL-2&7
G
Upregulated genes
IL-2&7 + IL-33 vs IL-2&7
IL-2&7 + LPS vs IL-2&7
135
141
72

Figure 6. RNA-seq analysis reveals that LPS upregulated genes significantly overlapped with those upregulated by IL-33 in human ILC2 cells . A. Heatmap showing the normalized mRNA expression level of all 10 human TLRs in human ILC2 cells from two donors. **B.** Volcano plot showing the up- and down-regulated genes in human ILC2 cells 6 hours after LPS treatment. **C.** Heatmap showing the differentially expressed genes (DEGs) in LPS-activated human ILC2 cells. **D.** Heatmap showing the selected cytokines genes in LPS-activated human ILC2 cells, in which genes related to type 2 immunity are highlighted in red. **E.** Dotplot of enrichment analysis with Kyoto Encyclopedia of Genes and Genomes (KEGG). **F.** GSEA analysis of DEGs upregulated by LPS and IL-33 in human ILC2 cells. **G.** Venn diagram depicting the overlapping and non-overlapping genes upregulated in human ILC2 cells stimulated with either IL-2&7 plus LPS or IL-2&7 plus IL-33, as compared to those treated with IL-2&7.

Figure 7

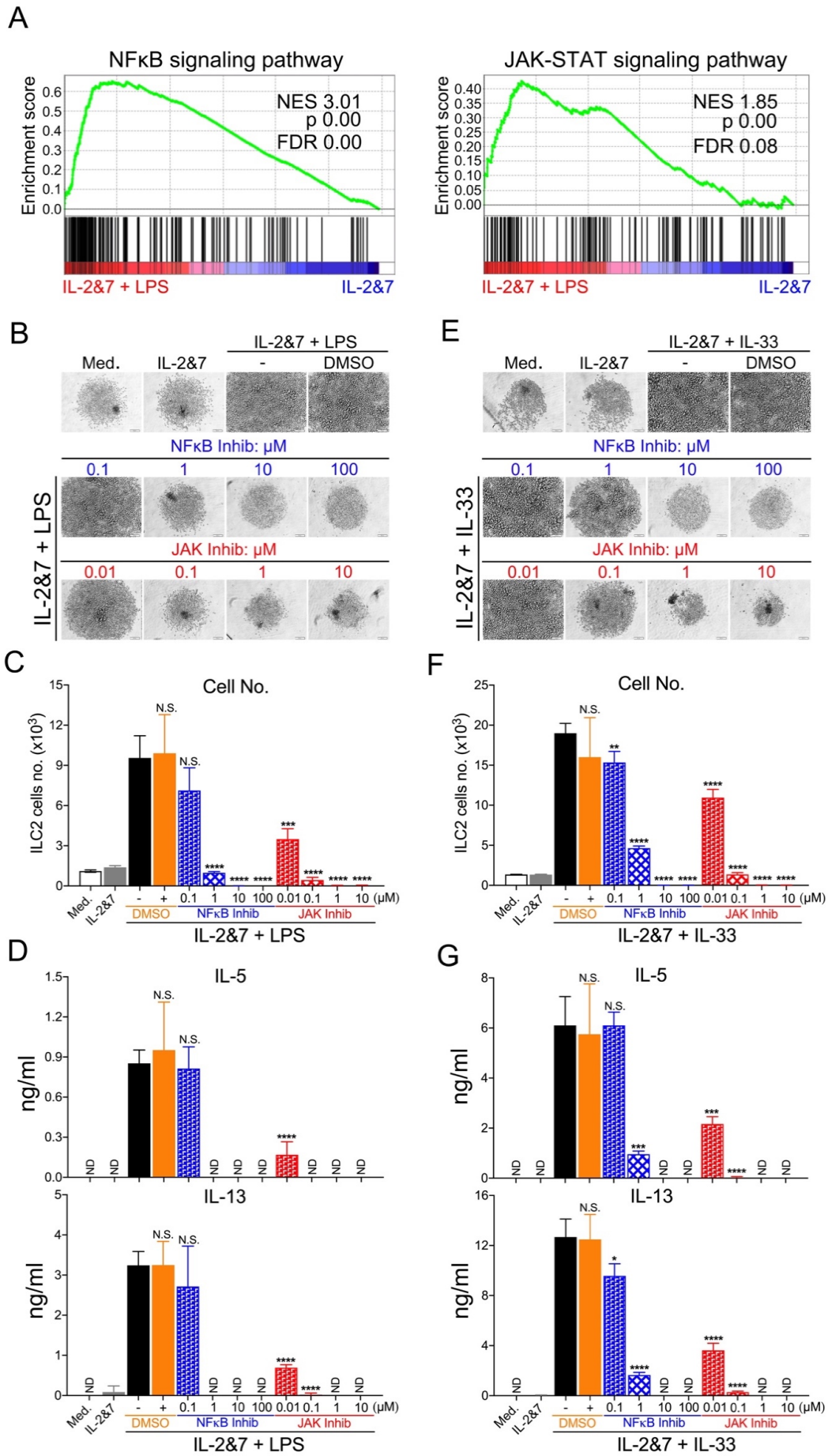
A
NFκB signaling pathway
Enrichment score
NES 3.01
p 0.00
FDR 0.00
IL-2&7 + LPS
IL-2&7
JAK-STAT signaling pathway
NES 1.85
p 0.00
FDR 0.08
B
Med.
IL-2&7
IL-2&7 + LPS
-
DMSO
NFκB Inhib: μM
0.1
1
10
100
JAK Inhib: μM
0.01
0.1
1
10
E
IL-2&7 + IL-33
C
Cell No.
ILC2 cells no. (x10³)
N.S.
DMSO
NFκB Inhib
JAK Inhib
(μM)
F
D
IL-5
IL-13
ng/ml
ND
G

Figure 7. NF-κB and JAK pathways contribute to the proliferation and cytokine production of LPS- and IL-33-stimulated human ILC2 cells. A. Venn diagram showing the DEGs in the NF-κB and JAK-STAT pathways in human ILC2 cells stimulated with IL-2&7 plus LPS, as compared to those treated with IL-2&7 **B.** Light microscopic images showing the growth of LPS-activated ILC2 cells in the presence of the increased concentration of NF-κB- and JAK- inhibitors, or DMSO. Each image represented one well in which 1,000 cells were initially seeded. Scale bar, 100μm. **C.** FACS showing the number of LPS-activated ILC2 cells in the presence of the increased concentration of NF-κB- and JAK- inhibitors, or DMSO. **D.** ELISA measuring the production of IL-5 and IL-13 by human ILC2 cells treated with LPS in the presence of the increased concentration of NF-κB- and JAK- inhibitors, or DMSO. **E.** Light microscopic images showing the growth of IL-33-activated ILC2 cells in the presence of the increased concentration of NF-κB- and JAK- inhibitors, or DMSO. Each image represented one well in which 1,000 cells were initially seeded. Scale bar, 100μm. **F.** FACS showing the number of IL-33-activated ILC2 cells in the presence of the increased concentration of NF-κB- and JAK- inhibitors, or DMSO. **G.** ELISA measuring the production of IL-5 and IL-13 by human ILC2 cells treated with IL-33 in the presence of the increased concentration of NF-κB- and JAK- inhibitors, or DMSO. (P value≥0.05 was considered statistically insignificant, N.S., unpaired t-test, * $p < 0.05$, ** $p < 0.01$, *** $p < 0.001$, **** $p < 0.0001$).

Figure 8

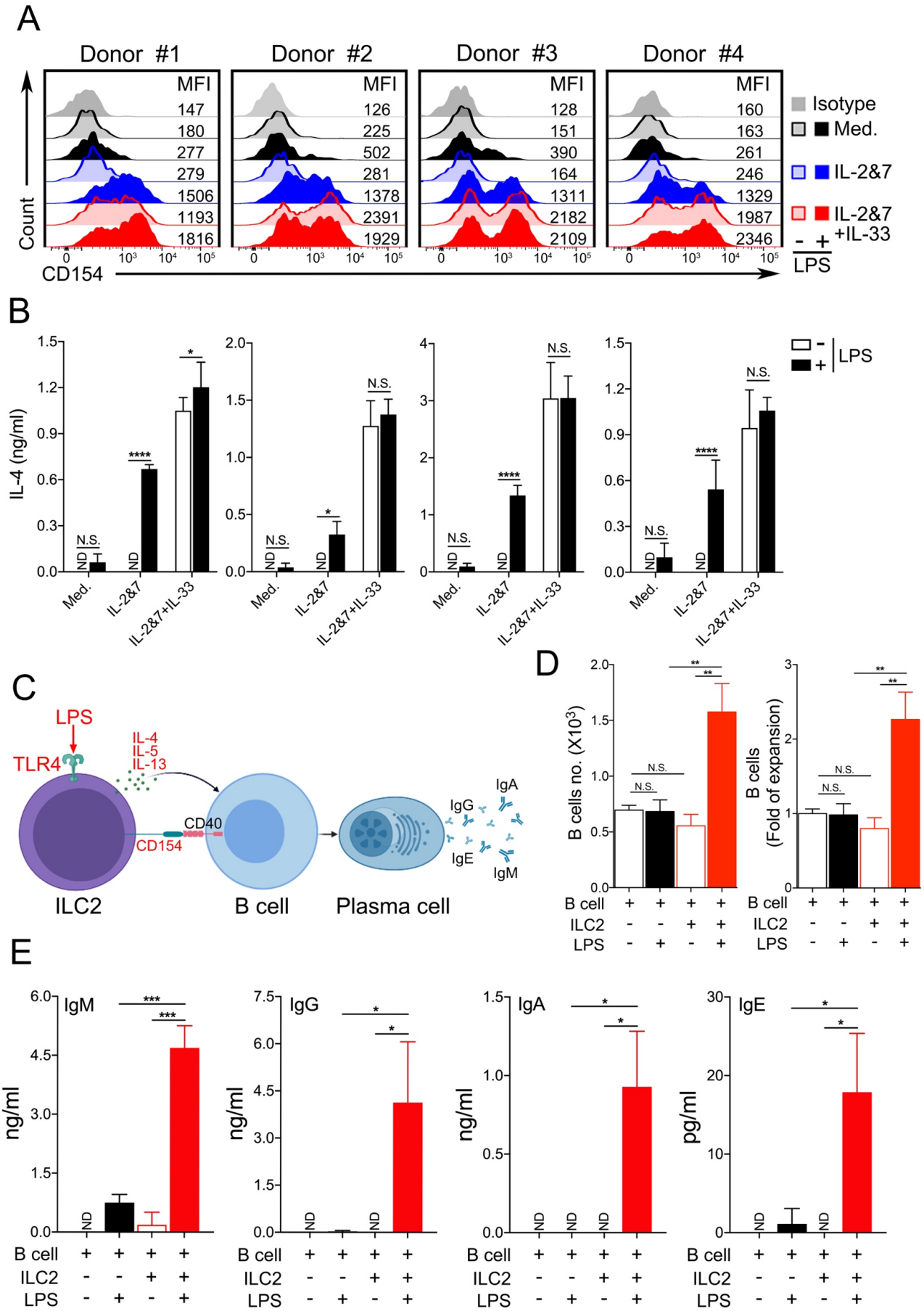
A
Donor #1
Donor #2
Donor #3
Donor #4
MFI
147
180
277
279
1506
1193
1816
126
225
502
281
1378
2391
1929
128
151
390
164
1311
2182
2109
160
163
261
246
1329
1987
2346
Isotype
Med.
IL-2&7
IL-2&7 +IL-33
- +
LPS
Count
CD154
B
IL-4 (ng/ml)
N.S.
ND
Med.
IL-2&7
IL-2&7+IL-33
LPS
C
LPS
TLR4
IL-4
IL-5
IL-13
CD40
CD154
ILC2
B cell
Plasma cell
IgA
IgG
IgE
IgM
D
B cells no. (X10³)
B cells (Fold of expansion)
B cell
ILC2
LPS
E
IgM
IgG
IgA
IgE
ng/ml
pg/ml

Figure 8. LPS-activated human ILC2 cells enhanced the proliferation and antibody production of B cells. A. FACS staining of CD154 proteins on the surface of human ILC2 cells from 4 individual donors treated with or without LPS as indicated. **B.** ELISA measuring the production of IL-4 by human ILC2 cells from 4 individual donors treated with or without LPS as indicated. **C.** A schematic diagram describing a working model for the interplay between LPS-activated ILC2 and B cells. **D.** FACS showing the increased number of B cells co-cultured with human ILC2 cells in the presence or absence of LPS. **E.** ELISA measuring the levels of antibodies (IgM, IgG, IgA and IgE) in supernatants of the co-cultured B and ILC2 cells in the presence or absence of LPS. (P value≥0.05 was considered statistically insignificant, N.S., unpaired t-test, * $p < 0.05$, ** $p < 0.01$, *** $p < 0.001$, **** $p < 0.0001$).

Figure 9

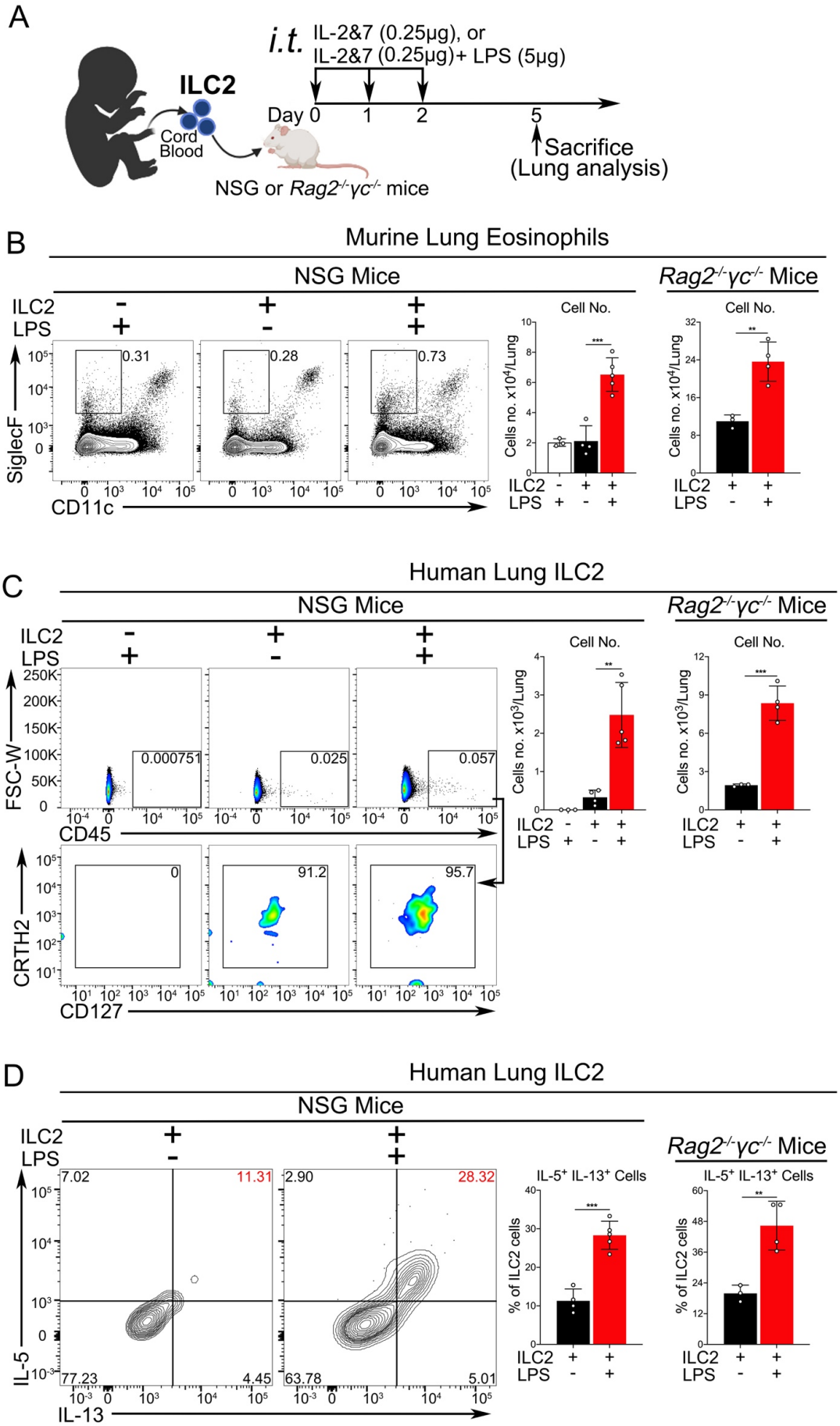
A
i.t. IL-2&7 (0.25μg), or
IL-2&7 (0.25μg)+ LPS (5μg)
ILC2
Cord Blood
Day 0 1 2 5
Sacrifice (Lung analysis)
NSG or Rag2-/-γc-/- mice
B
Murine Lung Eosinophils
NSG Mice
Rag2-/-γc-/- Mice
ILC2
LPS
SiglecF
CD11c
0.31
0.28
0.73
Cell No.
Cells no. x10⁴/Lung
C
Human Lung ILC2
NSG Mice
Rag2-/-γc-/- Mice
FSC-W
CD45
CRTH2
CD127
0.000751
0.025
0.057
0
91.2
95.7
Cell No.
Cells no. x10³/Lung
D
Human Lung ILC2
NSG Mice
Rag2-/-γc-/- Mice
IL-5
IL-13
7.02
11.31
77.23
4.45
2.90
28.32
63.78
5.01
IL-5+ IL-13+ Cells
% of ILC2 cells

Figure 9. LPS could induce human ILC2 cells-mediated eosinophilic lung inflammation in humanized mouse models. A. A experimental protocol for studying the activation of human ILC2 cells by LPS in two humanized mouse models. **B.** FACS showing the number of murine lung eosinophils in NSG or Rag2$^{-/-}\gamma c^{-/-}$ mice, which were reconstituted with human ILC2 and treated with or without LPS. **C.** Same as **B**, FACS showing the number of human ILC2 cells in NSG or Rag2$^{-/-}\gamma c^{-}$/- mice. **D.** Same as **B**, the percentage of IL5+IL13+-double positive human ILC2 cells in NSG or Rag2$^{-/-}\gamma c^{-/-}$ mice were analyzed by the intracellular staining. (P value≥0.05 was considered statistically insignificant, N.S., unpaired t-test, ** $p < 0.01$, *** $p < 0.001$,).

Figure S1

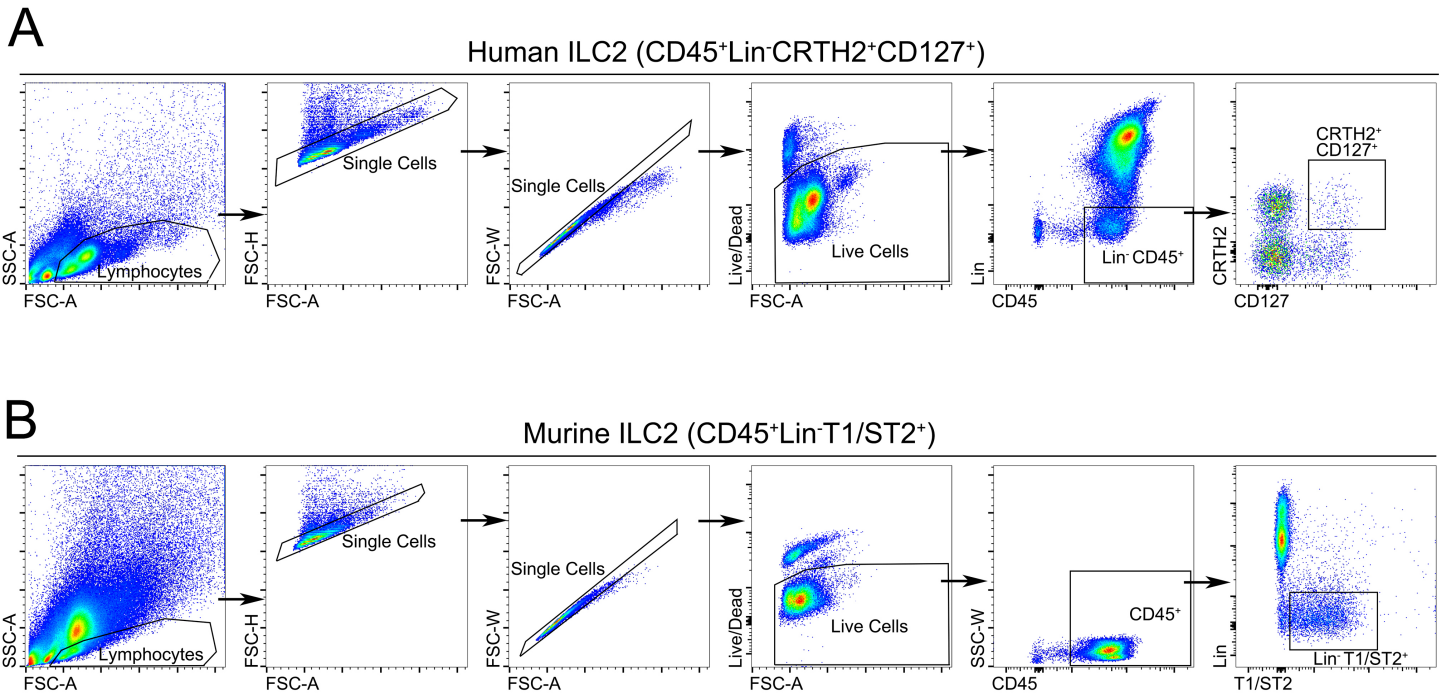

Fig. S1. Human and murine ILC2 gating strategy. A. Human ILC2s were isolated from peripheral blood of healthy donors PBMCs or umbilical cord blood samples CBMCs and stained with antibodies against CD45 and lineage markers. Human ILC2s were sorted by the BD FACSAria cell sorter as $CD45^{+}Lin^{-}CRTH2^{+}CD127^{+}$ cells. **B.** Murine ILC2s were isolated from mouse lungs treated with recombinant IL-33 protein (250ng/mouse, *i.t.*) and stained with antibodies against CD45 and lineage markers as described in the Materials and Methods. Murine ILC2s were sorted by the BD FACSAria cell sorter as $CD45^{+}Lin^{-}T1/ST2^{+}$ cells. The purity of sorted ILC2s was determined to be greater than 95%.

Figure S2

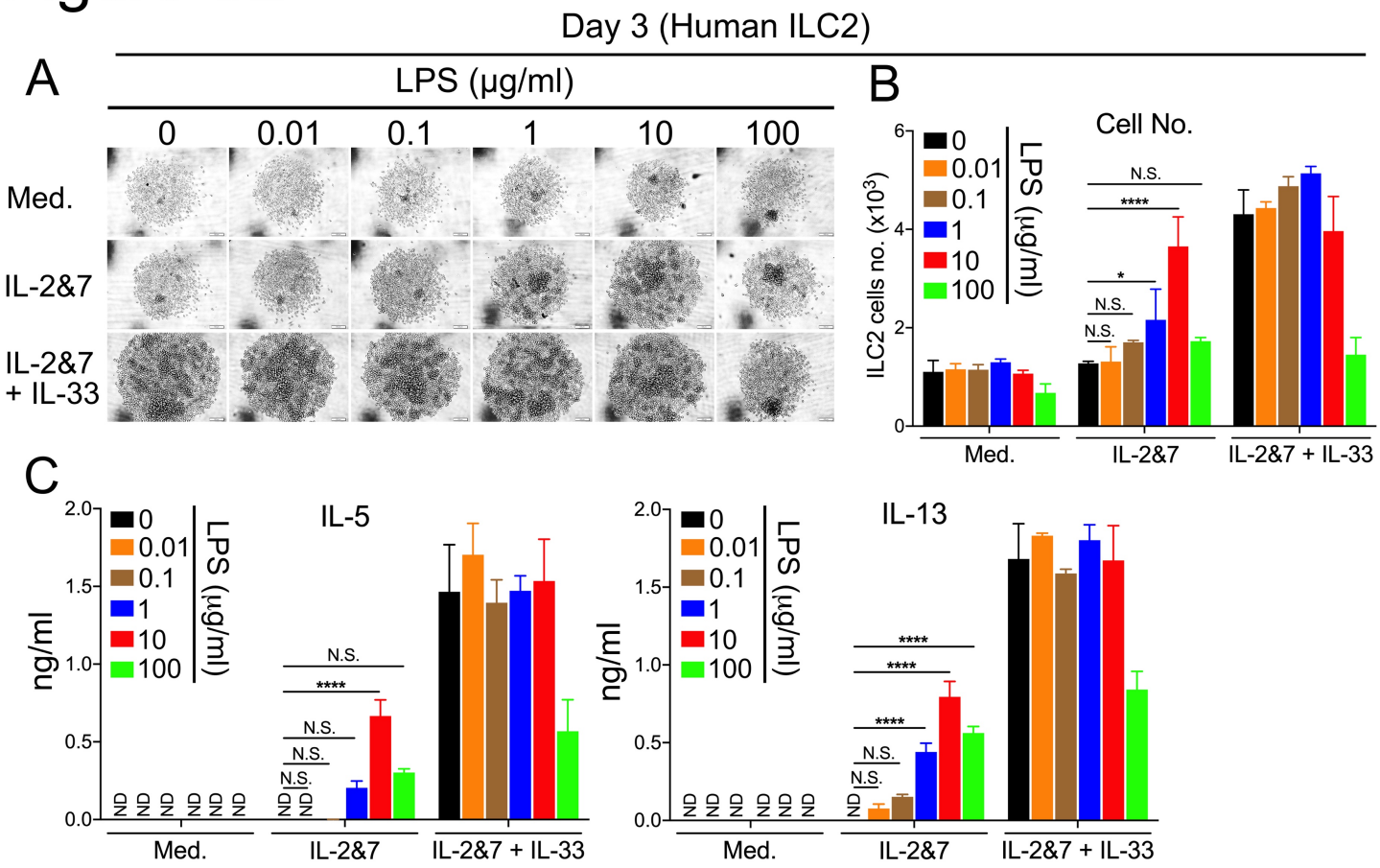

Figure S2. Analysis of LPS-stimulated human ILC2 cells on day 3. A. Light microscopic images showing the growth of ILC2 cells. FACS sorted human ILC2 cells were treated with the increased dose of LPS as indicated. Each image represented one well in which 1,000 cells were initially seeded. Scale bar, 100 μm. **B.** FACS showing the number of LPS-treated human ILC2 cells. **C.** ELISA measuring the production of IL-5 and IL-13 by human ILC2 cells treated with the increased dose of LPS. (P value≥0.05 was considered statistically insignificant, N.S., two-way ANOVA, * $p < 0.05$, **** $p < 0.0001$).

Figure S3

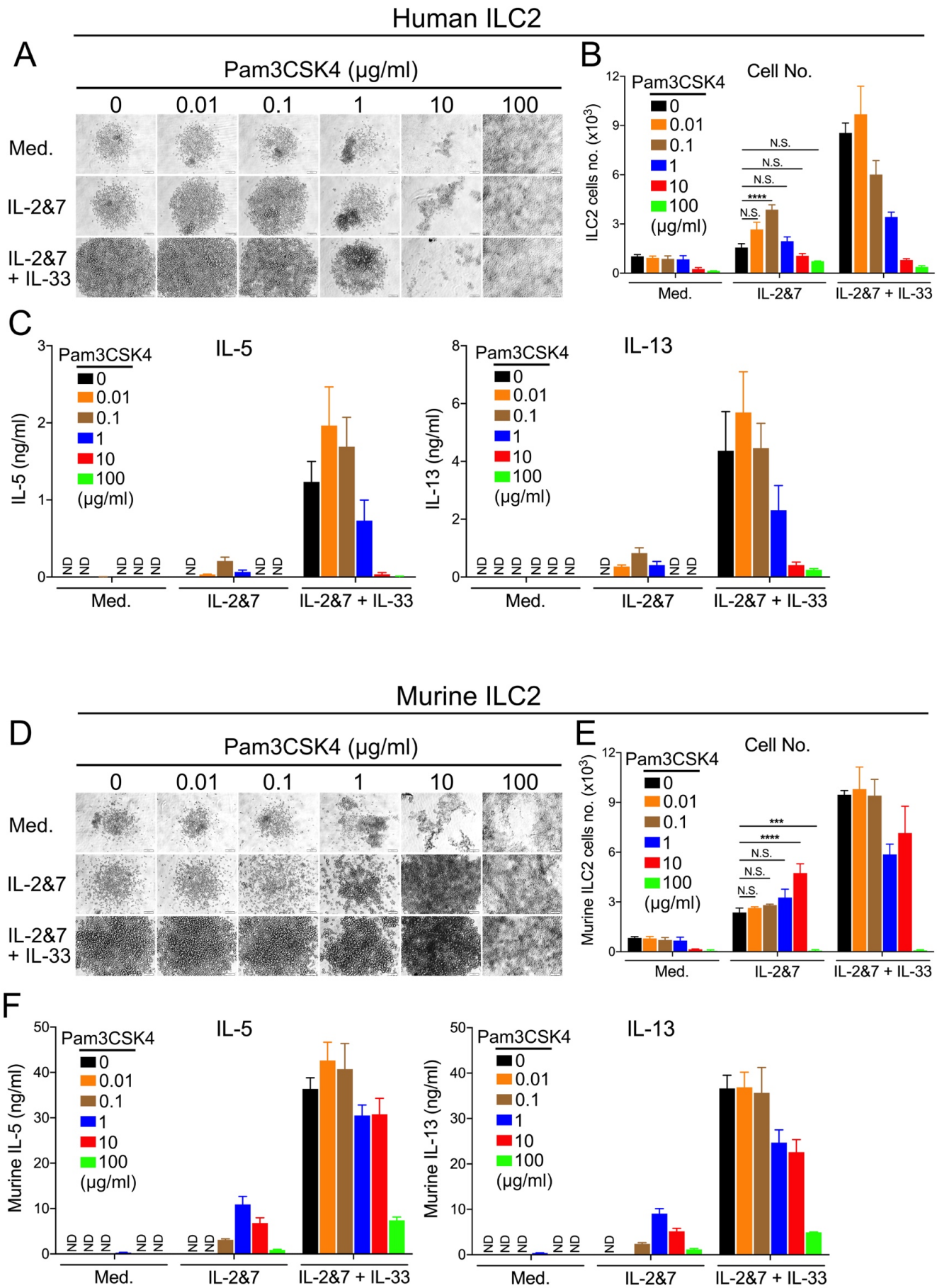
Human ILC2
A
Pam3CSK4 (μg/ml)
0
0.01
0.1
1
10
100
Med.
IL-2&7
IL-2&7 + IL-33
B
Cell No.
Pam3CSK4
0
0.01
0.1
1
10
100
(μg/ml)
ILC2 cells no. (x10³)
N.S.
N.S.
N.S.
****
N.S.
Med.
IL-2&7
IL-2&7 + IL-33
C
IL-5
IL-5 (ng/ml)
IL-13
IL-13 (ng/ml)
ND
Med.
IL-2&7
IL-2&7 + IL-33
Murine ILC2
D
E
Murine ILC2 cells no. (x10³)
***
****
N.S.
N.S.
N.S.
F
Murine IL-5 (ng/ml)
Murine IL-13 (ng/ml)

Figure S3. TLR2 agonist, Pam3CSK4, activates human or murine ILC2 cells at distinct concentrations. A. Light microscopic images showing the growth of human ILC2 cells stimulated with the increased doses of Pam3CSK4 as indicated. Each image represented one well in which 1,000 cells were initially seeded. Scale bar, 100μm. **B.** FACS showing the number of Pam3CSK4 -treated human ILC2 cells. **C.** ELISA measuring the production of IL-5 and IL-13 by human ILC2 cells treated with the increased dose of Pam3CSK4. **D**. Light microscopic images showing the growth of murine ILC2 cells stimulated with the increased doses of Pam3CSK4 as indicated. **E.** FACS showing the number of Pam3CSK4 -treated murine ILC2 cells. **F.** ELISA measuring the production of IL-5 and IL-13 by murine ILC2 cells treated with the increased dose of Pam3CSK4. (P value≥0.05 was considered statistically insignificant, N.S., two-way ANOVA, *** $p < 0.001$, **** $p < 0.0001$).

Figure S4

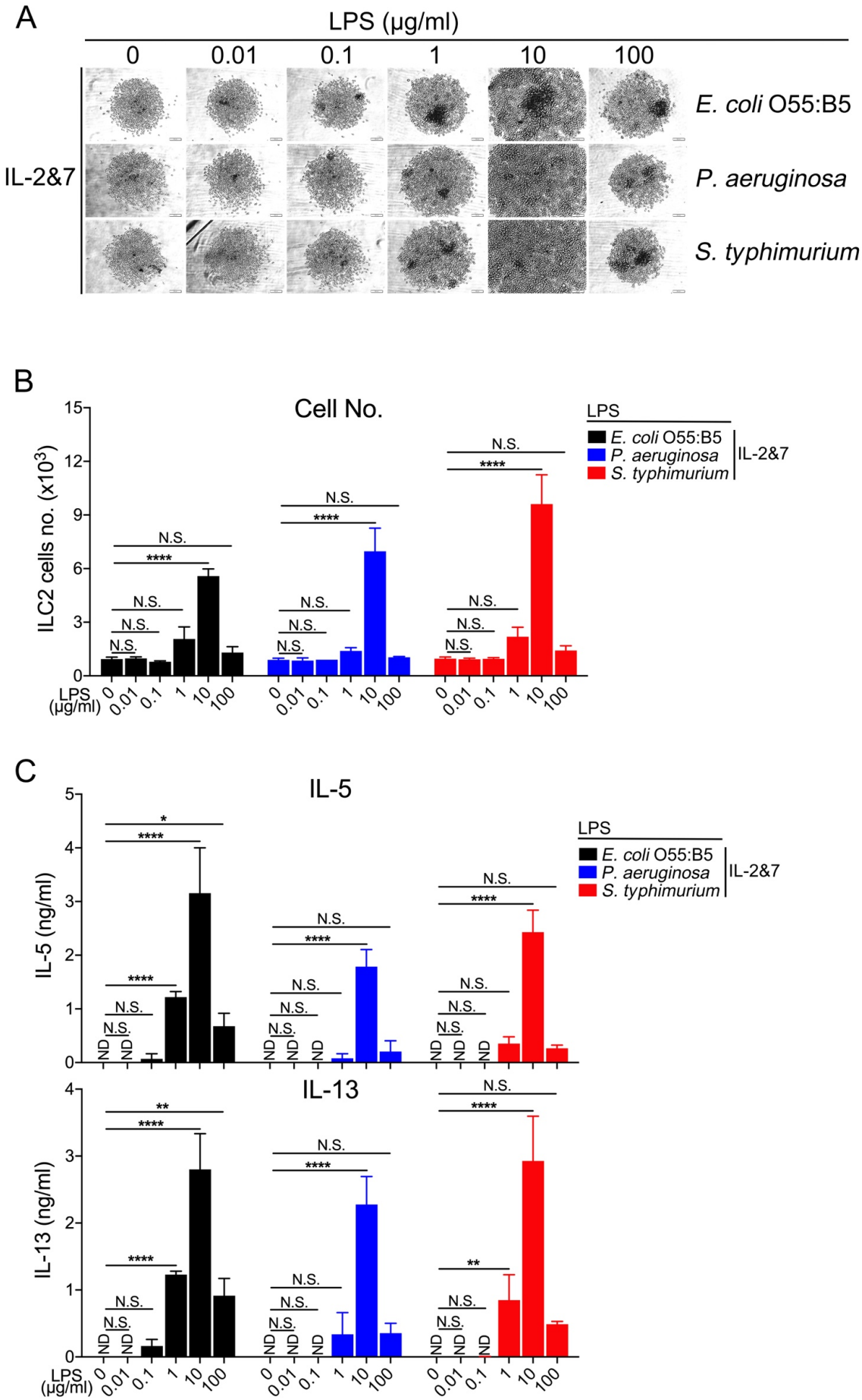
A
LPS (μg/ml)
0
0.01
0.1
1
10
100
IL-2&7
E. coli O55:B5
P. aeruginosa
S. typhimurium
B
Cell No.
ILC2 cells no. (x10^3)
LPS
E. coli O55:B5
P. aeruginosa
S. typhimurium
IL-2&7
N.S.
****
LPS (μg/ml)
C
IL-5
IL-5 (ng/ml)
IL-13
IL-13 (ng/ml)
ND
*
**

Figure S4. LPS from additional three Gram (-) bacterial species could stimulate the growth and cytokine production of human ILC2. A. Light microscopic images showing the growth of ILC2 cells treated with LPS isolated from *E. coli 055:B5*, *P. aeruginosa* and *S. typhimurium*. FACS sorted human ILC2 cells were treated with various LPS as indicated in a 96-well round-bottom plate for 5 days. Each image represented one well in which 1,000 cells were initially seeded. Scale bar, 100 μm. **B.** FACS showing the number of human ILC2 cells treated with various LPS as indicated. **C**. ELISA measuring the production of IL-5 and IL-13 by human ILC2 cells treated with various LPS as indicated. (P value≥0.05 was considered statistically insignificant, N.S., two-way ANOVA, * $p < 0.05$, ** $p < 0.01$, **** $p < 0.0001$).

Figure S5

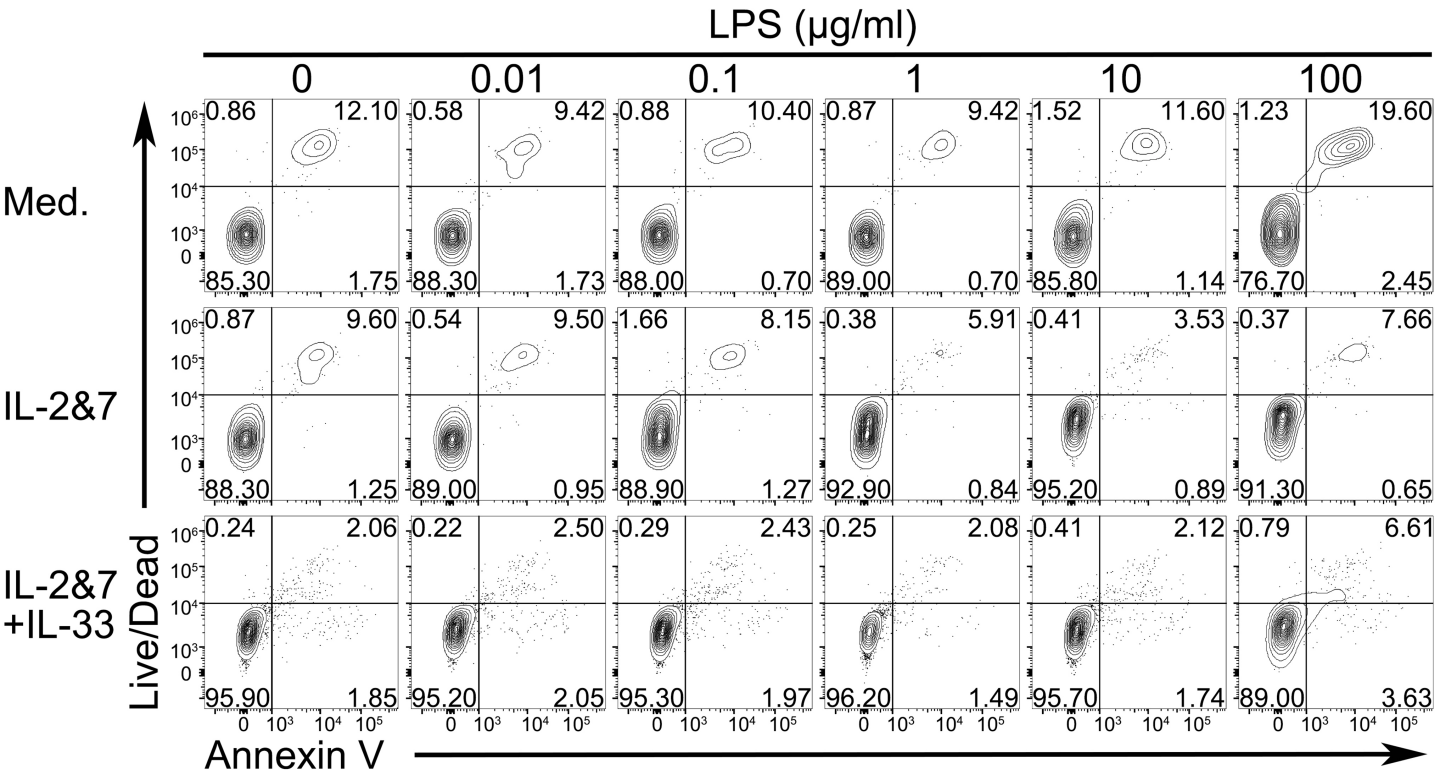

Figure S5. Cell death analysis of LPS-stimulated human ILC2 cells on day 3. FACS sorted human ILC2 cells were treated with the increased dose of LPS as indicated. FACS showing the cell death of LPS-treated human ILC2 cells.

Figure S6

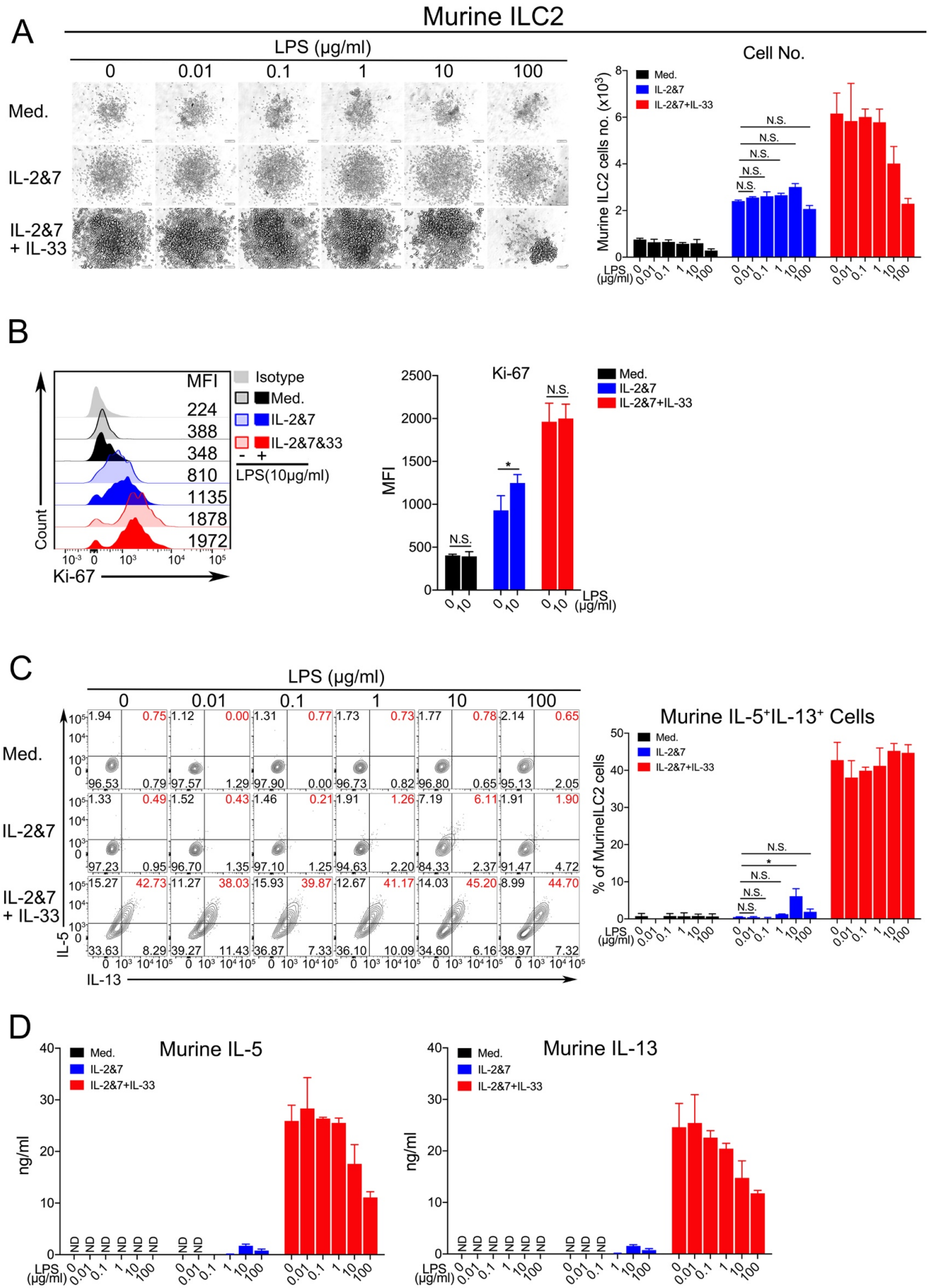
A
Murine ILC2
LPS (μg/ml)
0
0.01
0.1
1
10
100
Med.
IL-2&7
IL-2&7 + IL-33
Cell No.
Murine ILC2 cells no. (x10³)
Med.
IL-2&7
IL-2&7+IL-33
N.S.
LPS (μg/ml)
B
MFI
224
388
348
810
1135
1878
1972
Isotype
Med.
IL-2&7
IL-2&7&33
LPS(10μg/ml)
Count
Ki-67
Ki-67
MFI
N.S.
*
LPS (μg/ml)
C
LPS (μg/ml)
Med.
IL-2&7
IL-2&7 + IL-33
IL-5
IL-13
Murine IL-5⁺IL-13⁺ Cells
% of MurineILC2 cells
D
Murine IL-5
Murine IL-13
ng/ml
ND

Figure S6. The effect of LPS on stimulating murine ILC2 cells is weak. A. Light microscopic images showing the growth of murine ILC2 cells. FACS sorted murine ILC2 cells were treated with the increased dose of LPS as indicated. Each image represented one well in which 1,000 cells were initially seeded. Scale bar, 100μm (left panel). FACS showing the number of LPS-treated murine ILC2 cells (right panel). **B.** The LPS-treated murine ILC2 cells were analyzed with Ki-67 staining. The median fluorescence intensity (MFI) and quantification of Ki-67 were shown. The result is a representative of two independent experiments. **C**. The representative gating strategy and percentage of IL5+IL13+-double positive murine ILC2 cells treated with the increased dose of LPS were analyzed by the intracellular staining. **D.** ELISA measuring the production of IL-5 and IL-13 by murine ILC2 cells treated with the increased dose of LPS. (P value≥0.05 was considered statistically insignificant, N.S., two-way ANOVA, * $p < 0.05$).

Figure S7

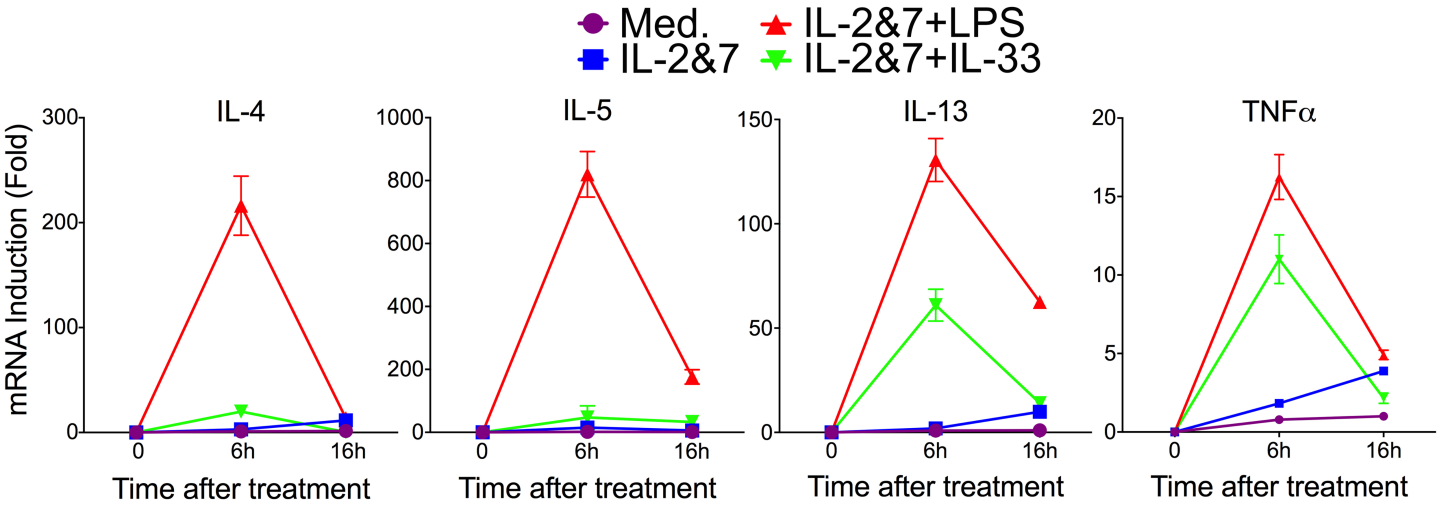

Figure S7. RT-qPCR analysis of selected gene expressions in LPS-stimulated human ILC2. Human ILC2 cells were collected at 0, 6 and 16 hours post LPS treatment. The mRNA expression of type 2 cytokines (IL-4, IL-5 and IL-13) and TNFα were measured with RT-qPCR.

Figure S8

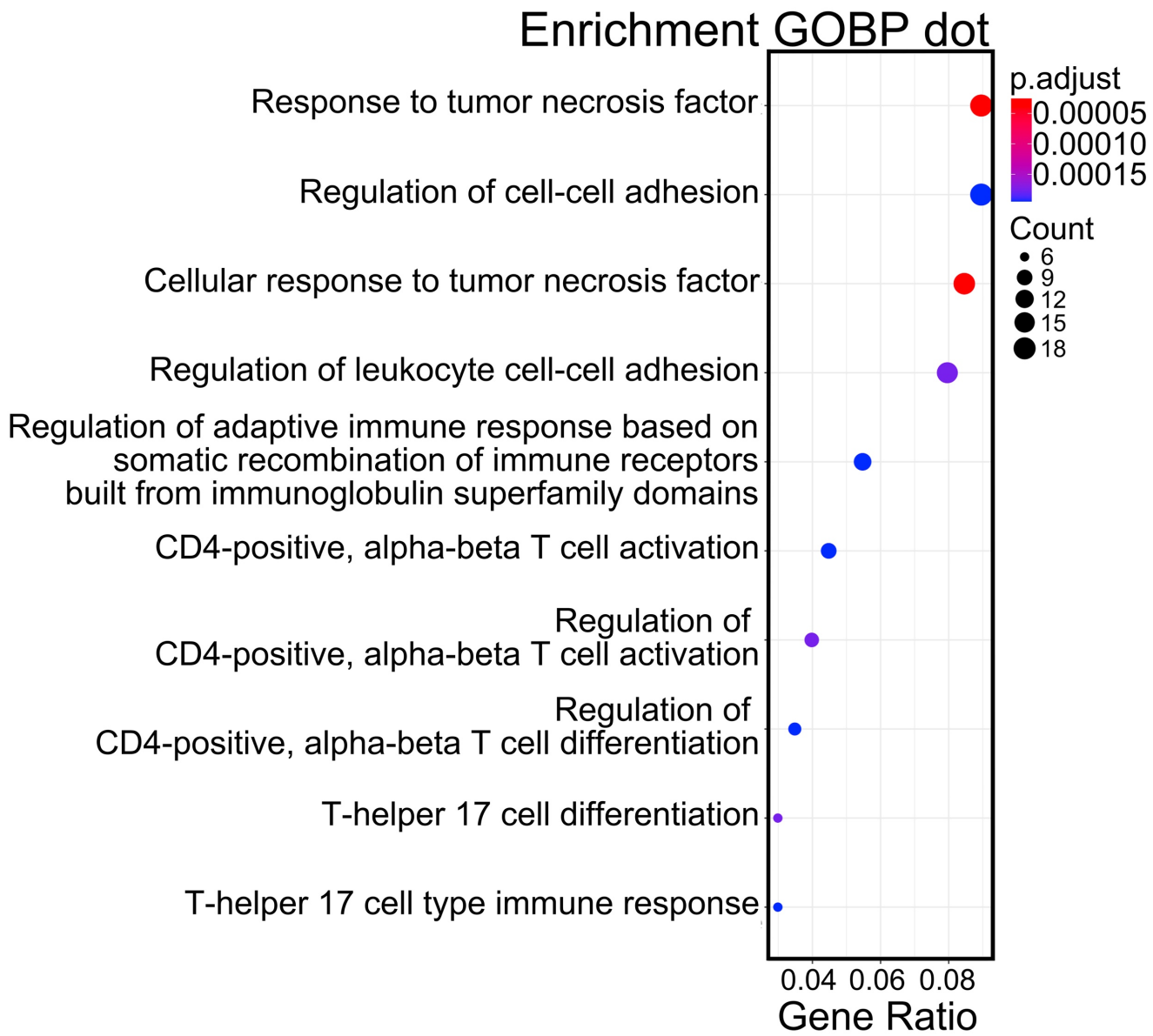

Figure S8. Dotplot of enrichment analysis with Gene Ontology biological process (GOBP).